MOUNT SINAI EXPERIENCE IN MIGRATING FROM RADIOACTIVE IRRADIATORS TO X-RAY IRRADIATORS FOR BLOOD AND MEDICAL RESEARCH APPLICATIONS

New York / September 2018

Mount Sinai

Table of Contents

	Page
Letter from Mount Sinai Leadership	**3**
Acknowledgement	**4**
Summary of Previous Studies	**5**
Radiobiology and Depth Dose Measurements. *Kamen J, Hill C*	**7**
Comparison of X-ray vs Cs irradiator for producing fibroblasts used to grow B cell lines in vitro. *Isaiah Peoples, Tina Yao, Denise Peace, Peter S. Heeger*	**13**
Comparison of X-ray vs Cs irradiator for the efficiency of transfer CD4+ T cells into B6 mice. *Lili Chen, Zhengxiang He, Glaucia Furtado & Sergio Lira*	**20**
X-ray irradiation, bone marrow transplantation, and composition of the donor-reconstituted murine immune system. *Verena van der Heide, Bennett Davenport and Dirk Homann*	**24**
Comparative analysis of X-ray vs 137Cs radiation in zebrafish embryos: cell death, organismal radiosensitivity and p53-dependence. *Renuka Raman, Yuanyuan Li and Samuel Sidi*	**31**
Comparison of effect of X-ray and Cs irradiation on PBMC in vitro. *Naoko Imai, Sacha Gnjatic*	**39**
Comparison of X-ray vs Cs-137 irradiation for producing mitotically-inactivated mouse embryonic fibroblasts to grow mouse embryonic stem (ES) cells. *Nika Hines, Pedro Sanabria and Kevin Kelley*	**44**
X-Ray Irradiation Is the Preferred Method of Irradiation for Tumor Cell Immunization. *Ananda Mookerjee and Thomas Weber*	**47**
Cancer Cell Organoid Core Experience in Transition to the X-ray irradiator. *Pamela Cheung, Ph.D. and Stuart Aaronson, M.D.*	**49**
Investigating the enhancing effects of combining radiation with oncolytic Newcastle Disease Virus (NDV) therapy in a murine melanoma model. *Gayathri Vijayakumar, Peter Palese, Peter Goff*	**50**
Comparisons of Using Cesium and X-ray as Sources of Irradiation in Blood Bank Operation *Jeffrey S. Jhang, MD and Suzanne Arinsburg, DO*	**52**
Conclusion and Recommendations	**58**

Letter from Mount Sinai Leadership

David L. Reich, MD

Dennis S. Charney, MD

We live in a dangerous world in which a major concern is the threat of terrorism, including the efforts of terror groups to obtain radioactive sources, such as cesium-137, as a component of a dirty bomb. Such a weapon could, depending upon its form and location, cause loss of many lives and billions of dollars in damage due to evacuation, relocation and decontamination.

In 2010, Mount Sinai decided to take steps to reduce the risk posed by radioactive irradiators that were used clinically for blood product irradiation and in our laboratory research, because of our location in New York City and our religious and cultural heritage.

Thus, when the new Hess Center for Biomedical research building needed an irradiator for research in 2013, Mount Sinai decided to purchase an X-ray irradiator as a step toward migrating to non-cesium technology. We collaborated with DOE-NNSA, performed comparison studies, and, as of January 2018, have migrated completely to alternative technology. In this report, we describe our experience in this migration and encourage other hospitals and research institutions to follow our lead.

We thank the Mount Sinai researchers and Blood Bank staff who collaborated to achieve success in a timely manner.

We all share a responsibility to protect our society from malicious use of radioactive materials.

David L. Reich, MD
President and Chief Operating Officer
The Mount Sinai Hospital

Dennis S. Charney, MD
Anne and Joel Ehrenkranz Dean
Icahn School of Medicine at Mount Sinai
President for Academic Affairs
Mount Sinai Health System

Acknowledgement

Jacob Kamen Ph.D.
Chief Radiation Safety Officer, Associate Professor of Radiology

I would like to express my deep appreciation to all who were instrumental in helping with Mount Sinai's successful migration from Cs-irradiators to X-ray irradiators.

Support from the leadership of Mount Sinai (Kenneth L. Davis, MD, Dennis S. Charney, MD, and David L. Reich, MD) was essential in the decision to adopt this alternative technology. Burton Drayer, MD, System Chair of Radiology; Kenneth Rosenzweig, MD, System Chair of Radiation Oncology; and Sally Strauss, Senior Vice President in the Legal Department, were very helpful in organizing initial meetings with Mount Sinai researchers and blood bank representatives to unify our effort to reduce the risk of terrorism by moving towards alternative technologies.

Collaboration with the Nuclear Threat Initiative (NTI), which is considered by many world leaders to be a world-class institution, has been very beneficial, especially with former Senator Sam Nunn, former UK Defense Secretary Lord Browne of Ladyton, former U.S. Energy Secretary Ernest J. Moniz, Executive Vice President Deborah Rosenblum, and Vice President Laura S. H. Holgate, Ambassador (ret.).

I would like to thank Reginald Miller, DVM, Dean for Research Operations and Infrastructure, for his constant communications with the researchers during the migration, as well as the staff of our animal research facility.

Ren-Dih Sheu, PhD, of Radiation Oncology, and Wen-Ya Hsu and Brandon Boswell of Radiation Safety were extremely helpful with the depth dose measurements. Collaboration with Mark Murphy of PNLL for depth dose measurement in the mouse phantom model was invaluable.

I am deeply thankful to Tim Burgunder and his staff of the Security department who provided essential services around the clock with both security enhancements and during the irradiator source removal process. The removal would not have been possible without the help of Detective Gail Ballantyne of the New York City Police Department. The help of NYCDOH Assistant Commissioner, Chris Boyd, is greatly appreciated.

Finally, I would like to gratefully acknowledge the help of the ORS (formerly GTRI) of the NNSA-DOE for their support during the security enhancement equipment phase when X-ray irradiators were not reliable. The help from the OSRP program of the U.S. DOE for the disposal of Cs-137 radioactive irradiators is appreciated. I also thank the support from the CRIP program of the US-DOE for X-ray Irradiators replacement.

Summary of Previous Studies

Jacob Kamen Ph.D.
Icahn School of Medicine at Mount Sinai, New York, NY, USA

In 2013, one study found that both Cs-137 and 320 kVp X-ray irradiators were both capable of destroying large numbers of bone marrow cells and splenocytes in mice. However they did find modest differences in the relative biological effectiveness (RBE) between the two irradiators. They found that the X-ray RBE relative to gamma rays for destroying bone marrow cells in vivo was > 1 while for destroying splenocytes was < 1. In contrast, dose-response relationships for reconstitution deficits in the bone marrow and spleen of C.B-17 mice at 6 weeks after radiation exposure were of the threshold type with gamma rays being more effective (lower threshold) in causing reconstitution deficits in both the bone marrow and spleen. [a]

In another study by the Insect Pest Control Laboratory of the Joint FAO/IAEA division of nuclear Techniques in Food and Agriculture, researchers found that using an X-ray irradiator was effective in reproductively sterilizing insects (SIT – Sterile Insect Technique). This indicates that the X-ray irradiator provides a practical alternative to self-shielded gamma irradiators for SIT. The x-ray irradiator they used fulfills the requirements of SIT programs for processing capacity, dose rate, dose uniformity and ease of use with some minor adjustments to irradiation geometry and canister size. [b]

Another recent paper concluded that both X-ray and Cs-137 irradiators provide similar results with regard to long-term peripheral blood reconstitution after bone marrow ablation. However, they did find some different physiologic responses with the two irradiators, specifically they found significant differences between the 2 sources in the establishment of B cell, myeloid, and T cell lineages. B cell reconstitution after exposure to a Cs-137 was greater than that after X-ray exposure at each dose level, whereas the converse was true for myeloid cell reconstitution. At the 1050- and 1100-cGy doses, mice irradiated by using the X-ray source demonstrated higher levels of T cell reconstitution but decreased survival compared with mice irradiated with the Cs-137 source. In addition, the Cs-137 source was associated with lower overall morbidity due to opportunistic infection. [c]

Additional authors investigated the replacement of Cs-137 irradiators with x-ray irradiators form a financial and pragmatic perspective. They found that replacing Cs-137 irradiator with a cabinet x-ray machine could be done with little to no loss in performance. The authors concluded that after disposing Cs-137 sources, the administrative overhead for the irradiator is likely to diminish and that the replacement costs are similar to purchase costs of Cs-137 irradiators. [d]

Another study was performed comparing X-ray and gamma irradiation of red blood cells (RBC). Although they found small differences in RBC membrane permeability between the gamma-irradiated and x-ray irradiated units, they concluded that these differences are not likely to be clinically significant. [e]

Recent working group recommendations published by University of California Systemwide Radioactive Source Replacement was printed in April 2018 and includes an RBE comparison table based on multiple research irradiator experiements. [f]

[a] A Comparison of in Vivo Cellular Responses to Cs-137 Gamma Rays and 320-KV X-Rays. *Scott BR1, Gott KM, Potter CA, Wilder J.*
[b] Characterization and dosimetry of a practical X-ray alternative to self-shielded gamma irradiators. *Kishor Mehta n, AndrewParker*

[c] Comparison of Cesium-137 and X-ray Irradiators by Using Bone Marrow Transplant Reconstitution in C57BL/6J Mice. *Brian W Gibson, Nathan C Boles, George P Souroullas, Alan J Herron, Joe K Fraley, Rebecca S Schwiebert,1 John J Sharp, and Margaret A Goodell*

[d] Replacement of 137Cs Irradiators with X-ray Irradiators. *Brian Dodd* and Richard J. Vetter*

[e] Comparison of X-ray vs. gamma irradiation of CPDA-1 red cells. *K. Janatpour, L. Denning, K. Nelson, B. Betlach, M. MacKenzie & P. Holland*

[f] MacKenzie, Carolyn, University of California Systemwide Radioactive Source Replacement Workgroup Recommendations, April 30, 2018.

Radiobiology and Depth Dose Measurements

Jacob Kamen Ph.D.[1], Colin Hill Ph.D.[2], Wen-Ya Hsu[1], Brandon Boswell[1]
[1]Icahn School of Medicine at Mount Sinai, New York, NY, USA
[2]Keck School of Medicine of University of Southern California

Radiation Dose

Radiation damage depends on the absorption of energy from the radiation and is approximately proportional to the mean concentration of absorbed energy in irradiated tissue. For this reason, radiation absorbed dose (D) is defined as the amount of ionizing energy absorbed (ΔE) per unit mass of irradiated material (Δm):

$$D = \frac{\Delta E}{\Delta m}$$

The unit for radiation absorbed dose in the SI system is called the gray (Gy) and is defined as follows: One gray is an absorbed radiation dose of one joule per kilogram. The gray is universally applicable to all types of ionizing radiation dosimetry— irradiation due to external fields of gamma rays, neutrons, or charged particles as well as that due to internally deposited radionuclides [i].

It is important to understand that the radiation absorbed dose concept is a macroscopic concept and is not intended for microdosimetry on the cellular or subcellular levels. Radiation absorbed dose has been found to be correlated with biomedical effects on the tissue, organ, and organism levels and thus is appropriate for radiation safety measurements and for medical diagnostic and therapeutic uses of radiation. The radiation absorbed dose concept implies that the absorbed energy is uniformly distributed throughout the entire mass of the tissue of interest. On the cellular and subcellular levels that are of interest to molecular biologists, the biological effects are proportional to the number and types of intramolecular bonds that are broken rather than to the concentration of absorbed energy within the cell. However there is a wealth of literature on effects on cells in culture that show absorbed dose for a variety of cellular level endpoints such as cell survival, mutations induced by radiation and neoplastic transformation induced by radiation is a good approximation and therefore relative biological effectiveness (RBE) is useful. An example, among many, by Spadinger and Palcic 1992 Int J. Radiat Biol.[ii], actually looked at the RBE for several radiations for two well-known cell lines on the tissue level; the number of such intramolecular breaks in the tissue is proportional to the radiation absorbed dose [iii].

- **Factors that affect Dose**

DOSE DISTRIBUTION One of the factors that affect the outcome from irradiation is the dose distribution in the irradiated specimen. During irradiation, photons and electrons enter a specimen and deposit energy. The flux of photons and electrons available for absorption decreases with depth since photons become absorbed as they penetrate the specimen. This creates non-uniformity in the dose distribution of the specimen, with a higher dose near the surface. In general, as photon energy increases the amount of attenuation through the specimen decreases. This means that higher energy photons typically produce a more uniform dose distribution. This effect is more pronounced for thicker specimens and for photon energies that are very different.

Non-uniformity can be reduced through a variety of ways. The specimen could be rotated with respect to the incident radiation so that the specimen is irradiated from multiple sides. This is the principle used justify turntable rotation in some Cs-137 irradiators or 'ferris-wheel'-like rotation in some blood irradiators and has been adopted in various forms as an option for some newer x-ray irradiators. Another method of increasing the dose uniformity is to surround the specimen with a block of photon reflective material. This method has been used in some research x-ray irradiators.

RBE The relative biological effectiveness (RBE) is defined as the ratio of the doses required by two radiations to produce the same biological effect. RBE is typically defined as the ratio of the dose required to produce a biological effect (e.g. skin reaction, death of mice…etc) for a given radiation type and energy (e.g. Cs-137 gamma rays) to the dose required to produce the same effect using a standard radiation type and energy (e.g. 250 keV x-rays).

$$\text{RBE} = \frac{\text{Dose of Standard Radiation}}{\text{Dose of Test Radiation}} \text{ for a given effect}$$

RBE depends on the radiation type and energy of both the standard and test radiation, and the biological effect being studied. Therefore RBE is inherently an empirical value which requires actual experimental data to quantify. In figure 4 below the general relationship between LET (Linear Energy transfer, keV/μm) and RBE is shown [ix].

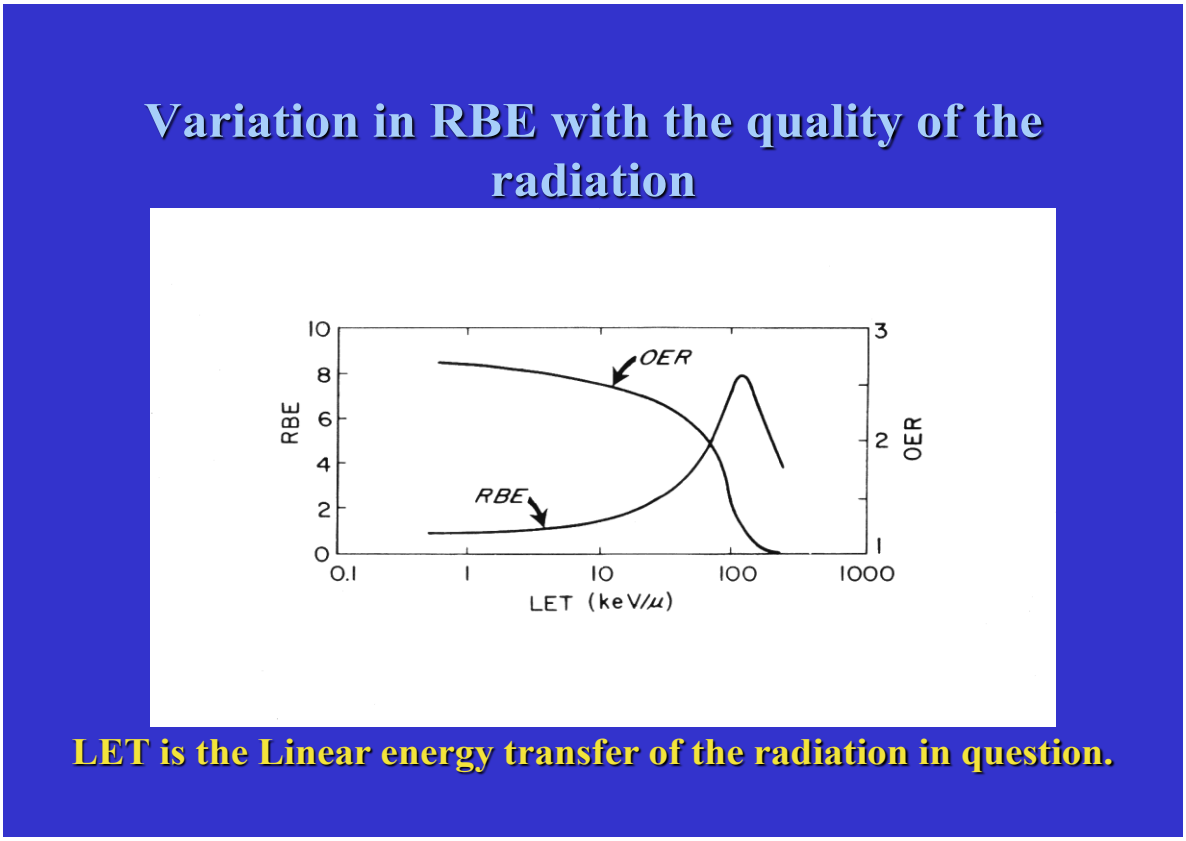

Figure 4. Variation of RBE with quality of the radiation. (Ref Hall E J. Radiobiology for the Radiologist). RBE has a value of 1 until about 10 keV/u then increases rapidly as energy increases.

The important take away from the relationship shown in figure 4 and in the list of LETs in figure 5 is that in the energy deposition region between 0.1 keV/u and almost 10 keV/u the RBE is 1. Cobalt 60 gamma radiation has an average LET of 0.2 kev/u while Cesium 137 radiation has an average LET of 0.91 keV/u and conventional 250 kv x-ray irradiation has an average LET of 2.0 keV/u. which all lie close to the LET of 1.0 keV/u on the log scale in figure 4 that has an RBE of 1.0. To be clear we are not talking here about x-rays below 55 kev that have significantly different RBEs and very different dose depth absorption characteristics. We are talking about energetic low LET radiations used to deposit dose as evenly as possible through everything from single cells to whole small animals.

Type of Radiation	LET (keV/μm)
Cobalt-60 gamma radiation	0.2
250 keV X-radiation	2.0
10 MeV protons	4.7
150 MeV protons	0.5
2.5 MeV α particles	166

Figure 5. Some average LET values for common ionizing radiation types.

Due to the complexity involved with performing RBE measurements for every possible radiation and every possible biological effect, the quantity "RBE" was simplified for the purposes of radiation protection to use a similar term called the "radiation weighting factor" (W_R). The biological effects of most interest to radiation protection are stochastic effects (e.g. cancer) produced by irradiating human tissue. For this particular biological effect, photons of different energies have approximately the same RBE, and therefore the tissue weighting factor is equal to 1 for photons of all energies. It should be noted that this does not imply that the RBE for all photon energies is the same, since RBE must always be defined in terms of the biological effect being observed. A sweeping conclusion that the RBE is independent of photon energy cannot be made on the basis that the RBE is approximately independent of photon energy for specifically stochastic effects observed in human tissue.[iv,v]

- **Repair**

Repair mechanisms also play key role radiation biology. Some biological effects caused by a dose of ionizing radiation may be repaired over time (e.g. DNA damage). In general, the longer the time between subsequent damage events, the increased likelihood of a successful repair. This principle is used in Radiation Oncology where a single large radiation dose is split into smaller fractions delivered over a longer period of time to allow for repair of healthy tissue (fractionation). The effect of repair mechanisms can also be seen within a single dose, where lower dose rates can have an increased repair. For instance, studies on dose–rate effects imply that there is a repair mechanism to correct genetic lesions. Animals exposed at low dose rates show mutation rates that are one-fifth to one-tenth the mutation rate observed at high dose rates. This dose–rate dependence implies a repair mechanism that is overwhelmed at high dose rates[vi]. Therefore, the dose rate used during irradiation is a factor that must be considered in evaluating the efficacy of irradiators. Decayed Cs-137 irradiators may have a lower dose rate which might impact the repair of cells. Generally repair becomes a significant factor if the dose rate falls below 0.5 to 5 cGy per minute depending on the endpoint under study [vii]. To be safe and for practical purposes it is probably not recommended to go below 50cGy per min (0.5 Gray/min).

Dose Variation

The dose distributions in Mount Sinai's irradiators were provided by the manufacturers at the commission of each irradiator. Figure 6 shows that the dose distribution in the x-ray irradiator (±3.8%) is more homogeneous than in the Cs-137 irradiator (±20%) at the location (level) for mice irradiation. There are large differences in source geometry, essentially between the point source (x-ray) and the line source (Cs-137 source). This is very important point because in cesium irradiators, the sample is rotated during the irradiation and if the mice move closer to the edge of the cage, then it will give completely different results than mice in the center of the cage. In an x-ray irradiator there is generally no rotation of samples although some newer machines are introducing rotating cages designed to give more dose consistency with depth in the x-ray beam.

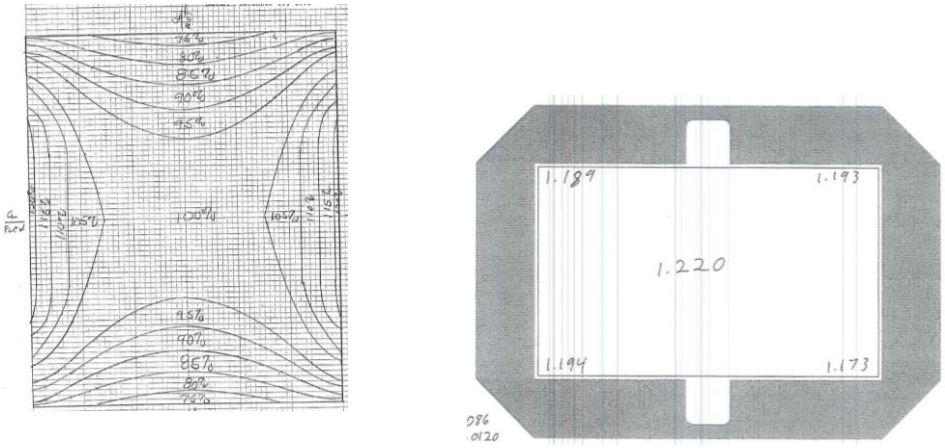

Figure 6. The dose distribution in the irradiators provided by the manufacturers. (Left) The isodose map in JL Shepherd Mark I-68 Cs-137 irradiator at location 3 measured with a film and provided by JL Shepherd. (Right) The Dose rate measurements in RS2000 x-ray irradiator at level 1 with RAD+ reflector.

Some cesium irradiators have two sources one below and one above the pancake shaped irradiation chamber. While this potentially avoids more dose on one side than the other it should be remembered that the 100% dose point is in the center between the two sources and as one gets closer to or touches the bottom of the chamber where the mice would normally be placed the dose can be 5 to 10% higher than the nominal dose rate measured in the center point. It is extremely important to measure (know) the absorbed dose rate at the location where your specimen is irradiated in the Cesium 137 irradiator before doing a comparison with a new X-ray machine. In an x-ray machine it is critical to measure dose distribution and dose rate at the center point of exposure as this absolutely varies with distance from the source and distance from the central axis of the x-ray beam. Using filtration and collimation x-ray machine manufacturers have improved the dose distribution over a significant area at a given distance as shown in the right panel of figure 6.

Percent Depth Dose (PDD) Measurement

British Journal of Radiology published supplement 25 which shows the results of Monte Carlo calculations of the Percent Depth Dose (PDD) curves.[viii]

We have measured the PDD curves using our own irradiators. The PDD curves were measured with EBT 2/ EBT 3 films sandwiched between different thicknesses of solid water phantom slabs and in small rodent phantoms in JL Shepherd Mark I-68 Cs-137 irradiator and RS2000 x-ray irradiator (160 kVp, 25 mA) respectively. The measurements in small rodent phantoms were performed by Mr. Mark Murphy from Pacific North National Lab (PNNL) using Mount Sinai's irradiators. The PDD measurements show very similar curves for 160 kVp x-ray 320 kVp x-ray and Cs-137 (662 keV) in both solid water phantoms and small rodent phantoms, particularly in the first 2 to 4 cm of depth in water that is relevant to cells, tissues and small whole animal exposures (Figure 7). The measurements in small rodent phantoms also show x-ray has more backscatter – contributing more doses and the Cs-137 field has significant Compton/scatter percentage. Please see below **Figure 7**.

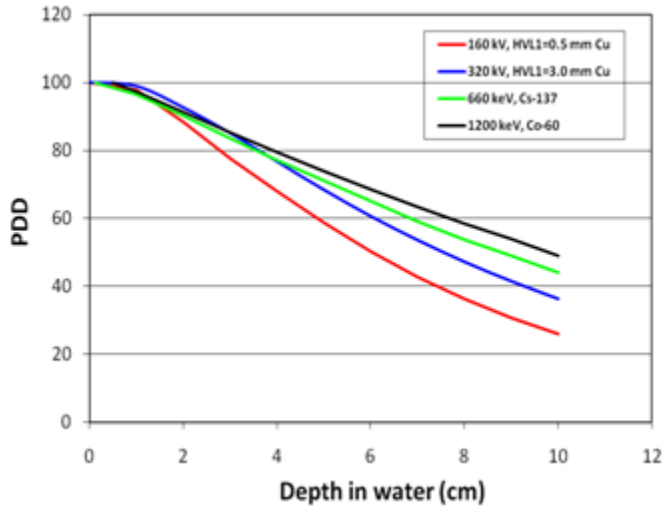

Figure 7. PDD plotted from data in BJR Supplement 25, for Three X-ray Qualities and for Cs-137 and Co-60. For all the following parameters apply: W=10 cm, SSD=50 cm[viii]

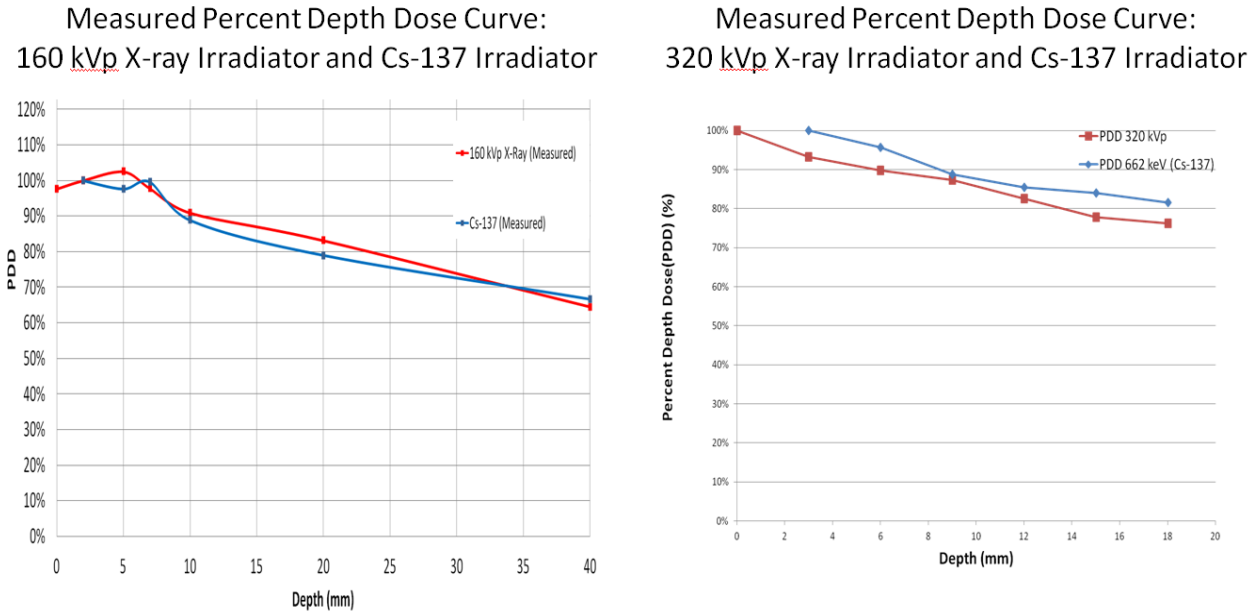

Figure 8. (Left) The PDD Curves comparison for 160 kVp x-ray (RS2000) and Cs-137 (JL Shepherd Mark I-68). The PDD curves measured with EBT 2 films sandwiched solid water phantoms. (Right) The PDD curves measurements comparisons for 320 kVp x-ray (X-RAD 320) and Cs-137 (JL Shepherd Mark I-68) .The PDD were measured with EBT 2 films sandwiched in small rodent phantoms.

References

[i] Cember H, Johnson TE. Introduction to Health Physics, 4th ed., New York: McGraw Hill. Page 203-204

[ii] Spadinger I1, Palcic B. The relative biological effectiveness of 60Co gamma-rays, 55 kVp X-rays, 250 kVp X-rays, and 11 MeV electrons at low doses. Int J Radiat Biol. 61(3):345-53. 1992.

[iii] Cember H, Johnson TE. Introduction to Health Physics, 4th ed., New York: McGraw Hill. Page 203-204

[iv] Relative Biological Effectiveness (RBE) Available at http://ozradonc.wikidot.com/rb:basic-rbe Accessed 20 June 2018.

[v] Biological aspects of heavy charged particle radiation therapy. Available at https://www.aapm.org/meetings/amos2/pdf/42-11865-82728-878.pdf Accessed 20 June 2018.

[vi] Cember H, Johnson TE. Introduction to Health Physics, 4th ed., New York: McGraw Hill. Page 317

[vii] Hill CK, Han A, Elkind MM. Possible Error-Prone Repair Of Neoplastic Transformation Induced By Fission Spectrum Neutrons. Br J Cancer Suppl. 6: 97–101. 1984.

[viii] BJR Suppl. 25 (1996) Central Axis Depth Dose Data for Use in Radiotherapy. British Journal of Radiology, Suppl, 25, London.

[ix] Hall, Eric, Radiobiology for the Radiologist, 7th ed., Philadelphia: Lippincott Williams & Wilkins.

Comparison of X-ray vs Cs irradiator for producing fibroblasts used to grow B cell lines in vitro

Isaiah Peoples, Tina Yao, Denise Peace, Peter S. Heeger

Translational Transplant Research Center

Icahn School of Medicine at Mount Sinai

Introduction

Our laboratory performs mechanistic and immune monitoring studies to support clinical trials in organ transplantation in humans. Among the assays that we perform is a measure of donor reactive T cell immunity; our data indicate that higher frequencies of donor reactive T cells that produce the cytokine interferon gamma (IFNg) associates with worse kidney transplant outcomes, i.e. higher rates of acute rejection episodes and worse kidney function at 1-2 years. [1-10]

To measure donor reactive IFNg producing cells in the peripheral blood we perform enzyme linked immunosorbent spot assays (ELISPOT assays) in which recipient mononuclear cells are mixed with donor derived B cells as donor stimulators and we quantify the numbers of IFNg producing cells 24 hours later. To standardize this assay we need to isolate and grow purified and activated B cell lines from each kidney transplant donor and then perform quality control assays to be sure that the B cell lines behave similarly[11]. This process is essential to standardize all assays among the hundreds of samples and patients that we study.

To expand B cell lines in vitro we stimulate them on a bed of fibroblasts that have been stably transfected such that they express a B cell stimulating molecule called CD154. These fibroblast feeder cells provide needed signals to stimulate the B cells but must not divide in the cultures, so they must be irradiated prior to use. The irradiation limits the ability of the fibroblasts to divide but does not kill them (which would prevent them from stimulating the B cells). Because the institution is transitioning from Cs irradiation to an X-ray irradiator we performed a series of experiments comparing various doses of X-irradiation to our gold standard Cs irradiation for preparation of the fibroblasts.

For each X-ray dose we analyzed percent survival of the fibroblasts, and then used the fibroblasts to stimulate B cells in parallel cultures. At the end of the expansion period we compared how many B cells were obtained and then assessed their activation status by measuring surface markers Class I HLA, Class II HLA, CD80 and CD86. Finally we used the resultant B cells as stimulators for ELISPOT assays using several donor PBMCs.

MATERIALS & METHODS

1. **B-Cell Isolation & Culture.** The PBMCs were separated from whole blood by Ficoll-Paque PLUS (GE Healthcare Bio-Sciences; Pittsburgh, PA) density gradient centrifugation. B Cells were isolated from peripheral blood mononuclear cells (PBMCs) by negative selection with the

Human B Cell Enrichment Kit (STEMCELL Technologies; Vancouver, BC) according to manufacturer instructions. B cells were grown on a feeder layer of the fibroblast in an Iscove's Modified Dulbecco's Medium (IMDM; GIBCO; Grand Island, NY) supplemented with 10% heat-inactivated Human AB serum (Gemini Bio-products; West Sacramento, CA), 1% penicillin-streptomycin (GIBCO), transferrin - 30mg/mL (Roche; Indianapolis, IN), human insulin - 50mg/mL (SIGMA, St. Louis, MO), gentamicin – 50mg/mL (Invitrogen; Grand Island, NY), plasmocin – 2.5mg/mL (InvivoGen; San Diego, CA) and IL-4 – 10ng/uL (Promega; Madison, WI). The B cells were incubated for 3-4d at 37°C, at 5% CO_2.

2. **Fibroblast Culture & Irradiation.** The murine NIH/3T3 Fibroblasts transfected with human CD40 ligand were cultured in a Roswell Park Memorial Institute Media (RPMI 1640; GIBCO), supplemented with 10% Fetal Bovine Serum (FBS; GE Healthcare Bio-Sciences; Pittsburgh, PA), 1% penicillin-streptomycin (GIBCO) and plasmocin – 2.5mg/mL (InvivoGen) in a T-75 flask and incubated at 37C, 5% CO_2. NIH/3T3 Fibroblasts were irradiated either with Cesium (Irradiator CORE at the Icahn School of Medicine at Mount Sinai) or X-ray using the RS 2000 Biological System (Rad Source; Suwanee, GA) in order to compare. Cells exposed to Cs irradiation were given a dose of 43Gy (control group). Cells exposed to X-ray irradiation (independent variables) were given various dosages, individually: 20Gy, 40Gy, 60Gy, 80Gy, 100Gy and 120Gy, respectively. After irradiation, fibroblasts were counted and 6.0×10^5 cells were plated in 15mL of RPMI-1640 media on 100mm dishes and incubated for at least 3-4hrs at 37°C, 5% CO_2 and serve as the feeder cell layer for the B cells.

3. **Flow Cytometry.** Flow cytometry data was acquired using a BD FACSCanto II (BD Biosciences; San Jose, CA), the FACSDiva software and analyzed using the Cytobank software. The following antibodies were used for staining: FITC- anti-HLA DR (BD Bioscience), PE-anti-CD19 (Invitrogen), PerCP-Cy5.5-anti-CD3 (BD Bioscience), APC-anti-HLA ABC (BD Bioscience) and BV510-anti-CD86 (BD Bioscience). FITC-anti-IgG_{2bk} (BD Bioscience), PE-anti-IgG1 (Miltenyi; San Diego, CA), PerCP-Cy5.5-anti-IgG_{1k} (BD Bioscience), APC-anti-IgG_{1k} (BD Bioscience) and BV510-anti-IgG_{1k} (BD Bioscience) were all used as isotype controls.

4. **ELISPOT.** Ninety-six well Millipore Multiscreen HTS IP sterile ELISPOT plates (Millipore; Billerica, MA) were coated with 100uL per well of the primary antibody, anti-IFNg (Endogen;) in PBS and incubated overnight at 4C. The ELISPOT plate was then blocked with 150uL of PBS + 1% BSA per well for 1h and then washed three times with sterile PBS. One-hundred thousand responder cells per well were stimulated with 100000 stimulator cells per well, unless otherwise stated. Phytohemagglutinin (PHA; SIGMA) was added to selected wells as positive controls at a final concentration of 10uL/mL of CTL-Test Media (CTL; Shaker Heights, OH). All assays were set at a final volume at 200uL per well. Control wells contained responder or stimulator cells with medium alone. After ELISPOT plate is incubated for 72h at 37C, 5% CO2 it is then washed three times with PBS and then four times with PBS-Tween20 (0.025%). After completion of washes 100uL of anti-IFNg-biotin (Endogen) at a 1:500 dilution in PBS-Tw + 1% BSA were added to each well and allowed to incubate at 4C overnight. The next day the plate is washed four times with PBS-Tw. Then 100uL of Streptavidin-HRP (BD Biosciences) at a 1:300 dilution with PBS-Tw + 1% BSA was added to each well and incubated for 4h at 4C. After 4h incubation

the plate is washed four times with PBS. The spots were then developed using AEC Substrate Set (BD Bioscience). The plate was then dried and the resulting spots were counted on a computer-assisted immunospot image analyzer (ELISPOT Reader; CTL).

5. **Statistical Analysis.** All statistical analysis was performed using GraphPad Prism (version 5 for Windows (GraphPad Software, Inc., La Jolla, CA). Results were compared using the Student's *t* test. A p-value ≤0.05 was considered significant. Error bars displayed are the mean of the group with SEM

Results and discussion

We observed that 20-60 Gy X-ray led to same fibroblast survival as Cs at 43 Gy (our standard), with doses of X-ray above that leading to increased fibroblast death (Fig 1). When we used the irradiated fibroblasts to stimulate B cells (Fig 2) we similarly observed X ray treatment 20-60 Gy had no effect on % growth of the B cells compared to the standard Cs 43 Gy. In contrast, higher doses of X-ray exposure led to lower % growth. When we analyzed the B cells for surface marker expression (Fig 3) as indicators of cell activation we did not detect differences among the various doses of Xray vs Cs with the occasional exception of lower levels in the B cells exposed to the highest doses of Xray (120 Gy). Finally, we used the B cells as stimulators in ELISPOT assays (Fig 4) we observed no differences in the T cell responses to the stimulating B cells when we used B cells grown on Cs treated fibroblasts (43 Gy) vs Xray treated fibroblasts exposed to 20-60 Gy. Based on these data we verified that fibroblasts exposed to 20-60 Gy function equivalently in our assays to fibroblasts exposed to 43 Gy of Cs source irradiator.

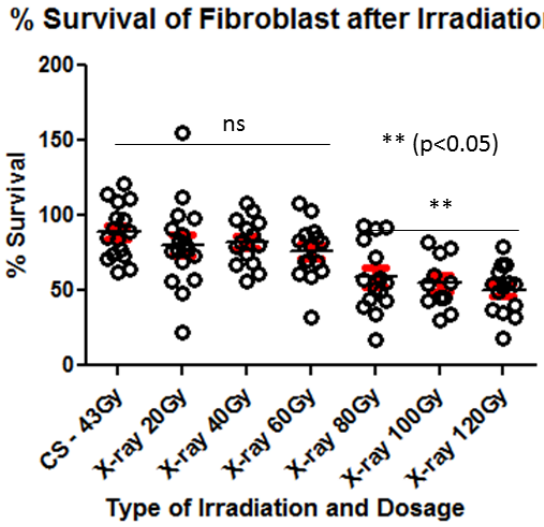

Figure 1 – Percent Survival of Fibroblast after irradiation. NIH 3T3 Fibroblast were split into several groups based on irradiation source (Cesium & X-ray) and dosage of irradiation (20gy – 120Gy; in increasing at 20Gy increments). After fibroblasts were irradiated they were then counted.

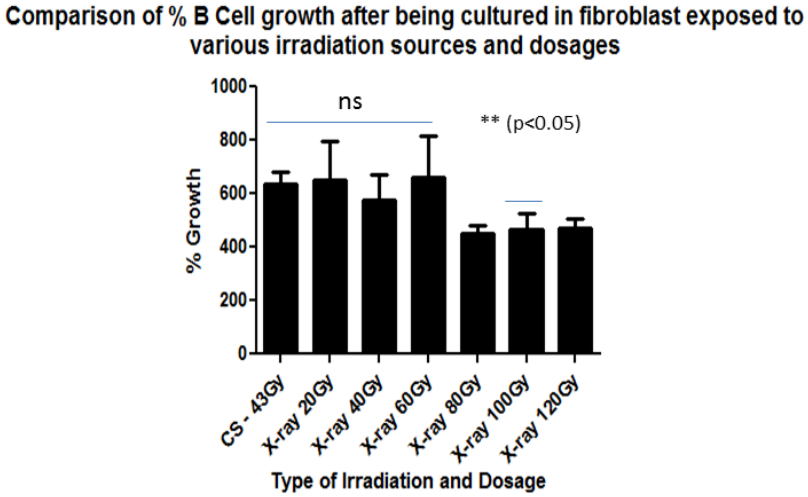

Figure 2 – Comparison of percent B Cell growth based on type of irradiation and dosage. B Cells isolated from PBMCs were seeded with feeder cells (NIH 3T3 Fibroblast) from both irradiation groups (Cs and x-ray). Each cell line was passaged after 3-4d, counted and the percentage change calculated.

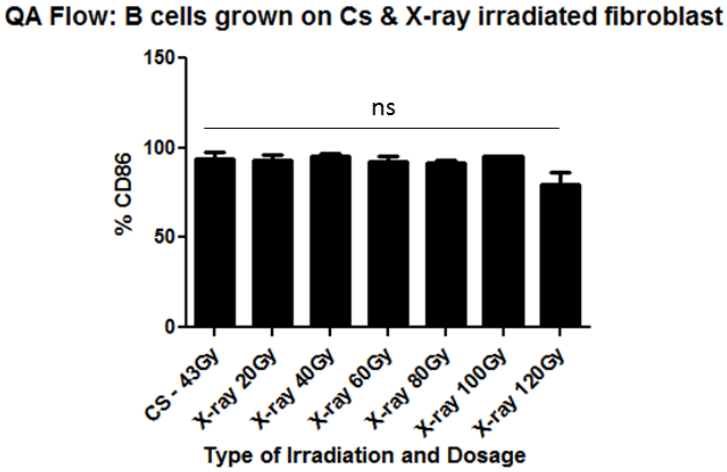

Figure 3b – Percent of cells with HLA-ABC on cell surface based on type of irradiation and dosage. B cells were stained with anti-HLA-ABC and analyzed using flow cytometry. Cells were gated to observe the cells with HLA-ABC on the cell surface. There was a noticeable difference in the b-cells seeded with fibroblast exposed to 120Gy but no significant difference was observed between the various groups. This was analyzed using the student's t-test comparing each experimental group to the control group (Cesium, 43Gy).

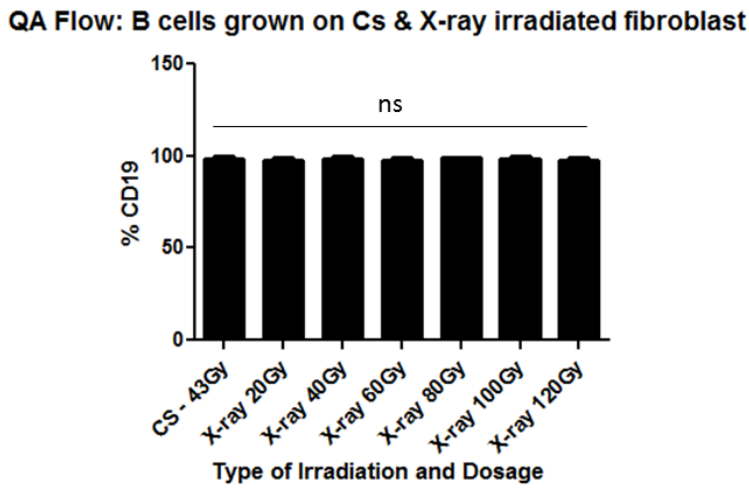

Figure 3c – Percent of cells with CD19 on cell surface based on type of irradiation and dosage. B cells were stained with anti-CD19 and analyzed using flow cytometry. Cells were gated to observe the cells with CD19 on the cell surface. No significant difference was observed between the various groups when compared to the control group (Cesium 43Gy) using the student's t test.

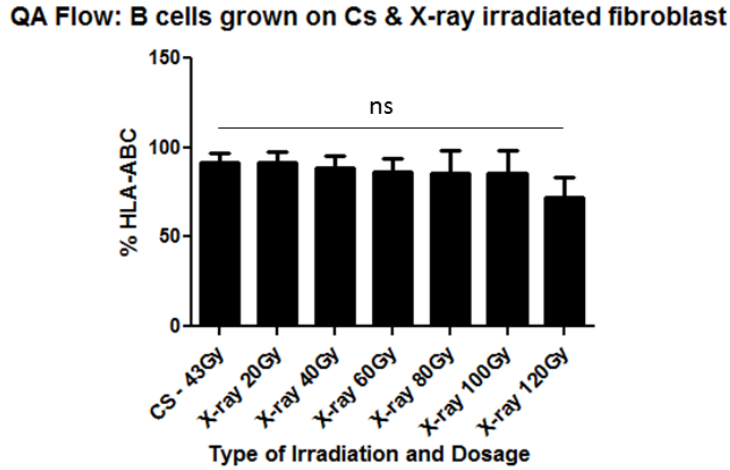

Figure 3d – Percent of cells with HLA-ABC on cell surface based on type of irradiation and dosage. B cells were stained with anti-HLA-ABC and analyzed using flow cytometry. Cells were gated to observe the cells with HLA-ABC on the cell surface. No significant difference was observed between the various groups when compared to the control group (Cesium 43Gy) using the student's t test.

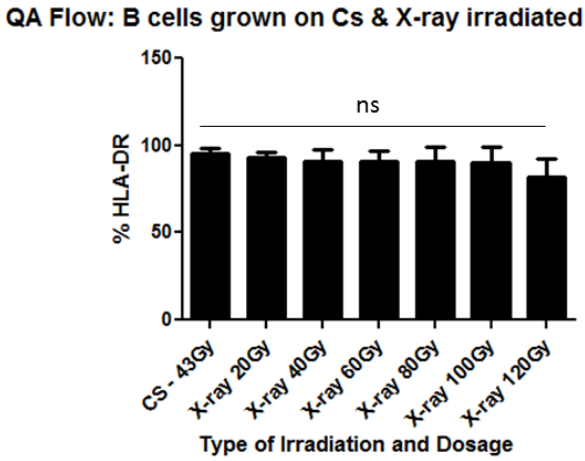

Figure 3e – Percent of cells with HLA-DR on cell surface based on type of irradiation and dosage. B cells were stained with anti-HLA-DR and analyzed using flow cytometry. Cells were gated to observe the cells with HLA-DR on the cell surface. No significant difference was observed between the various groups when compared to the control group (Cesium 43Gy) using the student's t test.

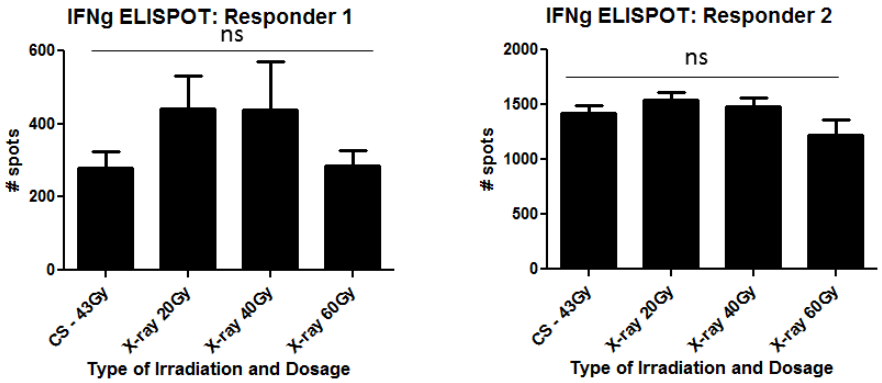

Figure 4– Number of IFNg-ELISPOT from PBMCs from 2 different responders stimulated with B cells prepared by x-ray irradiation ranging from 20-60Gy and compared to the control group (Cesium 43Gy). No significant difference was observed between the various groups when compared to the control group (Cesium 43Gy) using the student's t test.

References

1. Augustine JJ, Poggio ED, Clemente M, et al. Hemodialysis vintage, black ethnicity, and pretransplantation antidonor cellular immunity in kidney transplant recipients. *J Am Soc Nephrol*. 2007;18(5):1602-1606.
2. Augustine JJ, Poggio ED, Heeger PS, Hricik DE. Preferential benefit of antibody induction therapy in kidney recipients with high pretransplant frequencies of donor-reactive interferon-gamma enzyme-linked immunosorbent spots. *Transplantation*. 2008;86(4):529-534.
3. Augustine JJ, Siu DS, Clemente MJ, Schulak JA, Heeger PS, Hricik DE. Pre-transplant IFN-gamma ELISPOTs are associated with post-transplant renal function in African American renal transplant recipients. *Am J Transplant*. 2005;5(8):1971-1975.
4. Crespo E, Cravedi P, Martorell J, et al. Posttransplant peripheral blood donor-specific interferon-gamma enzyme-linked immune spot assay differentiates risk of subclinical rejection and de novo donor-specific alloantibodies in kidney transplant recipients. *Kidney Int*. 2017.
5. Faddoul G, Nadkarni GN, Bridges ND, et al. Analysis of biomarkers within the initial 2 years posttransplant and 5-year kidney transplant outcomes: results from Clinical Trials in Organ Transplantation-17. *Transplantation*. 2017.
6. Hricik DE, Augustine J, Nickerson P, et al. Interferon Gamma ELISPOT Testing as a Risk-Stratifying Biomarker for Kidney Transplant Injury: Results From the CTOT-01 Multicenter Study. *Am J Transplant*. 2015;15(12):3166-3173.
7. Hricik DE, Formica RN, Nickerson P, et al. Adverse Outcomes of Tacrolimus Withdrawal in Immune-Quiescent Kidney Transplant Recipients. *J Am Soc Nephrol*. 2015;26(12):3114-3122.
8. Hricik DE, Poggio ED, Woodside KJ, et al. Effects of cellular sensitization and donor age on acute rejection and graft function after deceased-donor kidney transplantation. *Transplantation*. 2013;95(10):1254-1258.
9. Hricik DE, Rodriguez V, Riley J, et al. Enzyme linked immunosorbent spot (ELISPOT) assay for interferon-gamma independently predicts renal function in kidney transplant recipients. *Am J Transplant*. 2003;3(7):878-884.
10. Poggio ED, Augustine JJ, Clemente M, et al. Pretransplant Cellular Alloimmunity as Assessed by a Panel of Reactive T Cells Assay Correlates With Acute Renal Graft Rejection. *Transplantation*. 2007;83(7):847-852 810.1097/1001.tp.0000258730.0000275137.0000258739.
11. Ashoor I, Najafian N, Korin Y, et al. Standardization and cross validation of alloreactive IFNgamma ELISPOT assays within the clinical trials in organ transplantation consortium. *Am J Transplant*. 2013;13(7):1871-1879.

Comparison of X-ray vs Cs irradiator for the efficiency of transfer $CD4^+$ T cells into B6 mice

Lili Chen, Zhengxiang He, Glaucia Furtado & Sergio Lira

Precision Immunology Institute

Icahn School of Medicine at Mount Sinai

Introduction

To examine the contribution of IL-23, the microbiota and diet to development of colitis, we created a novel mouse model in which IL-23 is conditionally expressed by fractalkine chemokine receptor positive (CX_3CR1^+) cells. CX_3CR1^+ macrophages and DCs are the main cells expressing IL-23 in the gut upon exposure to bacterial antigens [1,2]. Our results show that CX_3CR1^+-derived IL-23 expression triggers development of a colitis that is dependent on the microbiota and the diet, with diet-driven cycles of active disease (relapse/flares) followed by remission. The development of colitis in this model is dependent on the generation of a $CD4^+$ T cell response to the gut microbiota that is elicited by changes in the diet. Colitis-inducing $CD4^+$ T cells are found in the mesenteric lymph nodes (mLN) and large intestine during remission and are able to trigger disease when transferred to lymphopenic mice, but only upon diet modification [3]. Collectively, our experiments reveal a critical role for IL-23 in generation of a $CD4^+$ T cell population that is sensitive to modification of intestinal bacterial flora subsequent to a specific dietary manipulation.

To further investigate if the $CD4^+$ T cells obtained from *R23FR* mice could induce disease when transferred into sublethally irradiated B6 mice, we transferred MACS purified mLN $CD4^+$ T cells from d49 *R23FR* and *FR* mice to sublethally irradiated B6 mice.

MATERIALS & METHODS

6. **Diet treatment for the donor mice.** All mice were raised on the basal diet 5053, which was purchased from LabDiet (St. Louis, MO). The basal diet 2019 was purchased from Envigo (Madison, WI). Tamoxifen (500mg/kg) (Sigma) was added to the Envigo diet 2019. *R23FR* mice and control *FR* mice were fed with tamoxifen diet during the indicated times shown as Figure 1A. After each cycle of TAM treatment, animals were switched back to the basal diet 5053.

7. **T cell purification.** For $CD4^+$ T-cell isolation, mLNs were digested in collagenase as described previously [4]. $CD4^+$ T cells were enriched by positive immunoselection using CD4-(L3T4) microbeads (Miltenyi Biotec). The magnetic-activated cell sorting (MACS) purified $CD4^+$ T cells were used as donor cells in adoptive transfer experiments.

8. **CD_4 cell adoptive transfer.** B6 mice were sublethal irradiated either with Cesium (Irradiator CORE at the Icahn School of Medicine at Mount Sinai) or X-ray using the RS 2000 Biological System (Rad Source; Suwanee, GA). 4h after the irradiation, One million CD_4^+ from mLN enriched by using MACS-beads (Miltenyi Biotech) were transferred into sublethal irradiated *B6* recipient mice by intravenous (i.v.) injection.

9. **Optimization of the sublethal irradiation dose for the X-ray irradiator.** B6 mice exposed to X-ray irradiation were given various doses of: 500rad, 600rad and 700rad. After irradiation, mortality was recorded daily for 21 days.

10. **Flow Cytometry.** Flow cytometry data was acquired using a BD FACSCanto II (BD Biosciences; San Jose, CA), the FACSDiva software and analyzed using the Cytobank software. The following antibodies were used for staining: PE-anti-CD_3 (eBioscience), APC-cy7-CD_4 (eBioscience), APC-anti-CD_{45} (eBioscience) and PE-cy7-anti-CD11b (eBioscience).

11. **Histology.** Tissues were dissected, fixed in 10% phosphate-buffered formalin, and then processed for paraffin sections. Five-micrometer sections were stained with hematoxylin and eosin (H&E) for histological analyses. All the sections were evaluated for a wide variety of histological features that included epithelial integrity, number of goblet cells (mucin production), stromal inflammation, crypt abscesses, erosion, and submucosal edema. Severity of disease was then classified based on a modified version of the Histologic Activity Index as described before[5]. Briefly, the disease score in the large intestine was calculated as follows: grade 0: absence of epithelial damage, focal stromal inflammation or regenerative changes; grade 1: crypt abscesses in less than 50% of the epithelium. Diffuse stromal inflammation and/or regenerative changes; grade 2: crypt abscesses in more than 50% of the epithelium and focal erosion or cryptic loss. Diffuse and accentuated crypt distortion with stromal inflammation; grade 3: Pan-colitis, diffuse erosion and ulcers.

12. **Statistical Analysis.** All statistical analysis was performed using GraphPad Prism (version 5 for Windows (GraphPad Software, Inc., La Jolla, CA). Differences between groups were analyzed with Student's *t* tests or nonparametric Mann-Whitney test. Statistical tests are indicated throughout the Figure legends. Differences were considered significant when $p < 0.05$ (NS, not significant, * $p < 0.05$, **$p < 0.01$, ***$p < 0.001$), and levels of significance are specified throughout the Figure legends. Data are shown as mean values ± SEM throughout.

Results and discussion

We have generated a novel mouse colitis model by inducing the expression of IL-23 in the intestinal DC and macrophages (R23FR mice, FR mice were used as negative control) and our previous results show that CD4 cells are essential for the disease development. To investigate if the $CD4^+$ T cells obtained from *R23FR* mice could induce disease when transferred into sublethally irradiated B6 mice, we transferred MACS purified mLN $CD4^+$ T cells from d49 *R23FR* and *FR* mice to sublethally irradiated B6 mice (700rad Cs) and treated them with different diets for 21 days (**Figure 1A**). We observed comparable frequencies of donor $CD4^+$ T cells ($CD45.2^+$) in the blood of the recipients (**Figure 1B**). Transfer of control *FR* $CD4^+$ T cells did not elicit colitis in sublethally irradiated B6 mice, regardless of the diet regimen (Figure 1C). Transfer of *R23FR* $CD4^+$ T cells to sublethally irradiated B6 mice that were fed with diet 5053 also did not promote disease. However sublethally irradiated B6 mice that received *R23FR* $CD4^+$ T cells and were fed with 2 cycles of 2019 diet developed severe colitis (**Figure 1C**).

However, when we repeated this experiment, our Cs source irradiator was terminated and we only could use the X-ray source irradiator. So we switched to the X-ray source irradiator. Using the Cs source all the mice survived until d21 after receiving 700rad. However, using 700rad from the X-ray source we observed high mortality (15/20) before d12 (**Figure 2A**). Analysis of the peripheral blood of a few surviving animals showed that these animals lacked CD45 cells in the blood (**Figure 2B**), which suggested that the mice that received 700rad X-ray died from BM depletion. This experiment suggested that the irradiation doses from Cs and X-ray were different. We then performed additional experiments to optimize the sublethal irradiation dose for the X-ray source. We found that the 500rad X-ray is the safest dose, all the mice survived until d21 (**Figure 2A**).

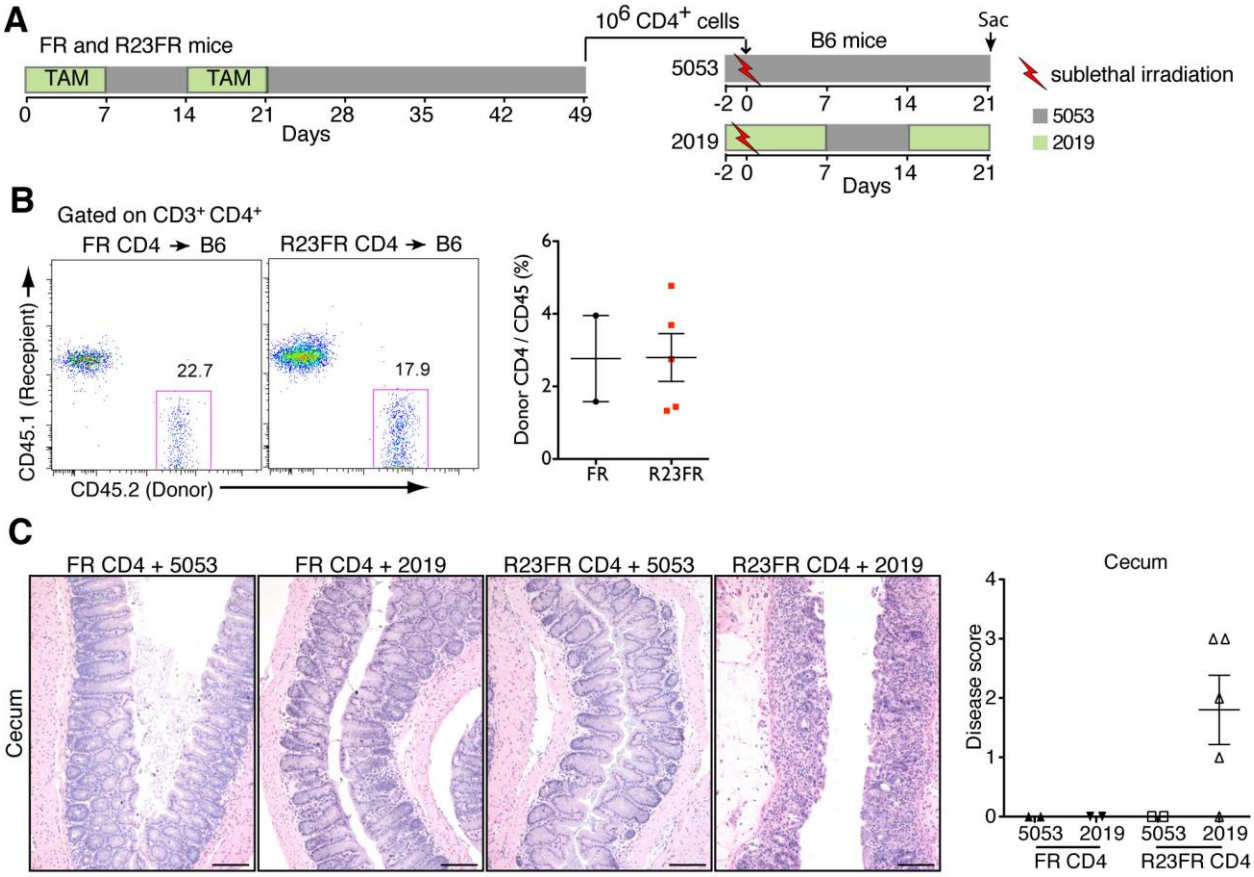

Figure 1. IL-23-induced CD4$^+$ T Cells Drive Inflammation in Adoptively Transferred sublethally irradiated B6 Mice. (A) Experimental setup for adoptive transfer of mLN CD4$^+$ T cells from of *R23FR* or *FR* mice into sublethal irradiated B6 mice (700rad Cs). (B) FACS analysis of donor CD4$^+$ T cells (CD45.2$^+$) in the blood of recipient sublethal irradiated B6 mice injected with CD4$^+$ T cells fed with 2019 diets. (C) Representative H&E staining (left) and histological scores (right) of the cecum of sublethal irradiated B6 mice that received *R23FR* and *FR* mice CD4$^+$ T cells fed with different diets.

References:

1. Farache, J., Zigmond, E., Shakhar, G. & Jung, S. Contributions of dendritic cells and macrophages to intestinal homeostasis and immune defense. *Immunol Cell Biol* **91**, 232-239 (2013).
2. Oppmann, B.*, et al.* Novel p19 protein engages IL-12p40 to form a cytokine, IL-23, with biological activities similar as well as distinct from IL-12. *Immunity* **13**, 715-725 (2000).
3. Lili Chen, Z.H., Alina Cornelia Iuga, Sebastião N. Martins Filho, Jeremiah J. Faith, Jose C. Clemente, Madhura Deshpande, Anitha Jayaprakash, Jean-Frederic Colombel, Juan J. Lafaille, Ravi Sachidanandam, Glaucia C. Furtado,Sergio A. Lira. Diet Modifies Colonic Microbiota and CD4+ T cell Repertoire to Trigger Flares in a Novel Model of Colitis Induced by IL-23. *BioRxiv* (2018). doi: https://doi.org/10.1101/262634.
4. He, Z.*, et al.* Epithelial-derived IL-33 promotes intestinal tumorigenesis in Apc (Min/+) mice. *Scientific reports* **7**, 5520 (2017).
5. Gupta, R.B.*, et al.* Histologic inflammation is a risk factor for progression to colorectal neoplasia in ulcerative colitis: A cohort study. *Gastroenterology* **133**, 1099-1105 (2007).

X-ray irradiation, bone marrow transplantation, and composition

of the donor-reconstituted murine immune system

Verena van der Heide, Bennett Davenport and Dirk Homann

Diabetes Obesity Metabolism Institute & Precision Immunology Institute;

Icahn School of Medicine at Mount Sinai, New York, NY

ABSTRACT

The ongoing transition from gamma to X-ray irradiators as a preferred source for ionizing radiation in biomedical research requires an adjustment of experimental protocols, including those employed for the generation of murine bone marrow chimeras. Building on recent work in the field, we demonstrate here that lethal X-ray irradiation and subsequent bone marrow transplantation allows for effective immune system reconstitution with donor-derived myeloid cells, B cells, and over time also $CD4^+$T cells in the absence of adverse health effects. In contrast, composition of the $CD8^+$T cell compartment is compromised by the presence of residual host $CD8^+$T cells, and preliminary studies indicate that improved reconstitution with donor $CD8^+$T cells may be achieved with a higher energy X-ray source. Thus, optimized protocols for the generation of bone marrow chimeras with a complete donor-derived immune system remain to be developed.

INTRODUCTION

Ablation of the murine bone marrow (BM) through ionizing radiation and subsequent BM transplantation for reconstitution with a donor-derived immune system constitutes a fundamental tool in experimental immunology (1, 2). Although lethal irradiation with ~900-1200 cGy delivered through either ^{137}Cs or X-ray sources has long been used for this purpose (1), ^{137}Cs irradiation protocols appear to be the preferred option due to reliable destruction of recipient BM, effective repopulation with donor BM-derived hematopoetic cells (>90%) as well as excellent survival and long-term health of the chimeras. However, few studies have directly compared the impact of ^{137}Cs *vs.* X-ray irradiation on overall chimera health and reconstitution efficiency (3-6), and potential differences pertaining to the reconstitution of particular immune cell subsets are only beginning to come into focus (7). Here, using the established approach of recipient and donor

mice congenic at the CD45 locus to easily distinguish host- and donor-derived leukocytes (1), Gibson *et al.* observed a slightly but significantly reduced reconstitution with donor leukocytes after 1,100 cGy X-ray (~90%) *vs.* ^{137}Cs (~95%) irradiation, a skewed distribution of major hematopoetic cell subsets, and a decreased survival of the chimeras (7). In regards to the composition of the reconstituted peripheral immune system, X-ray irradiation comparatively favored outgrowth of myeloid and T cells at the expense of B cells but the data presented in the report did not reveal the extent to which individual immune cell populations harbored host- rather than donor-derived subsets (7). Building on this study and using our own experience with ^{137}Cs irradiation-generated chimeras as a historical reference (8, 9), we set out to determine in greater detail how immune cell subset reconstitution in BM chimeras is shaped by the use of X-ray irradiation protocols.

METHODS

Mice and BM chimera generation.

C57BL6/J (B6; CD45.2/CD90.2), congenic B6.CD45.1 (B6.SJL-*Ptprc*^{a} *Pepc*^{b}/BoyJ) and congenic B6.CD90.1 (B6.PL-*Thy1*^{a}/CyJ) mice were purchased from The Jackson Laboratory and housed together in the Icahn School of Medicine vivaria in the Hess and/or Icahn buildings. BM chimeras were constructed using protocols adapted from previously published approaches (8). In brief, mice were fasted for 24h prior to irradiation using two different X-ray sources and cumulative dosages as detailed below. Donor BM was harvested from femurs and tibias, T cells were depleted using αCD4/αCD8 magnetic beads and an autoMACS cell separator (Miltenyi), and 3-5x10^{6} T cell-depleted BM cells were transferred i.v. into irradiated recipients; as based on our prior experience, we refrained from providing acidified water or antibiotics to the BM chimeras. Alternatively, we performed lineage depletion with αCD5, αCD45R, αCD11b, αGr-1, αLy-6B.2 and αTer-11 antibodies (Miltenyi) prior to transfer of 3.5-8.5x10^{5} stem cell-enriched BM cells into irradiated recipients. All procedures involving laboratory animals were conducted in accordance with the recommendations in the “Guide for the Care and Use of Laboratory Animals of the National Institutes of Health”, the protocols were approved by the Institutional Animal Care and Use Committees (IACUC) of the Icahn School of Medicine at Mount Sinai (IACUC-2014-0170), and all efforts were made to minimize suffering of animals.

X-ray irradiators and irradiation protocols.

We used two different X-ray sources for the administration of lethal irradiation dosages to murine BM recipients, a RS 2000 Biological System Irradiator (RadSource, USA) and a X-Rad

320 Biological Irradiator (Precision X-ray Inc., USA). The RS 2000 Biological System Irradiator operates with a default setting of 160 kV and 25 mA, its irradiation chamber has five height levels available that accommodate trays for the support of containers with biological specimen, six circles on the trays correspond to respective radiation field sizes at a given height, and a RAD+ reflector is employed to make dose distribution more uniform (***Fig.1A/B***). This set-up allows for the delivery of five different dose rates, and dose rates at each level were measured during initial installation as well as annual preventive maintenance; in addition, we assess the dose rate at the bottom level on a monthly schedule to assure that delivery of irradiation proceeds at the quoted rates. The average dose rate inside the RAD+ reflector and specimen container was 1.25 Gy/min with a uniform beam of 3.8% variation only in the field as measured with an electrometer (Model Accu-Dose/2086, Radcal Corporation, USA), an ionization chamber (model 10X6-06-3, Radcal Corporation, USA). For irradiation of mice, plexiglass containers containing the mice were placed in the RAD+ reflector at the bottom level of the chamber as recommended by the manufacturer and exposed to a cumulative dosage of 1,200 cGy (2x600 cGy delivered ~3h apart).

The X-Rad 320 Biological Irradiator, acquired only in 2017, provides more flexibility in settings since the kV settings can be adjusted from 5 kVp to 320 kVp, and the mA settings can range from 0.5 to 45 mA. There are different options of filters that can be used, and an adjustable platform can hold biological specimen at different heights. A parallel plate ionization chamber is integrated into the x-ray head to provide dose measurement and exposure control to specimens placed inside the cabinet. A variable collimator is installed to provide 0 to 20cm x 20cm (at 50 cm SSD) X-ray field size and the illuminated radiation exposure field indicator (***Fig.1C/D***). With these accessories, irradiation settings can be adjusted and optimized according to desired outcomes. For the present study, we maintained the default one setting as recommended by the manufacturer (320 kVp, 12.5 mA, SSD = 50cm, and filter 2 for small animal irradiation). Mice placed individually into chambers of a plexiglass pie carousel were irradiated using cumulative dosages of 1,320 cGy or 1,100 cGy (delivered in split dosages administered ~3h apart). Dose rates and the uniformity were previously measured with an electrometer (T10010, PTW Freiburg, Germany), an ionization chamber (TN30013, PTW Freiburg, Germany); and the dose rate and distribution within the irradiation field is confirmed once per year during the preventive maintenance.

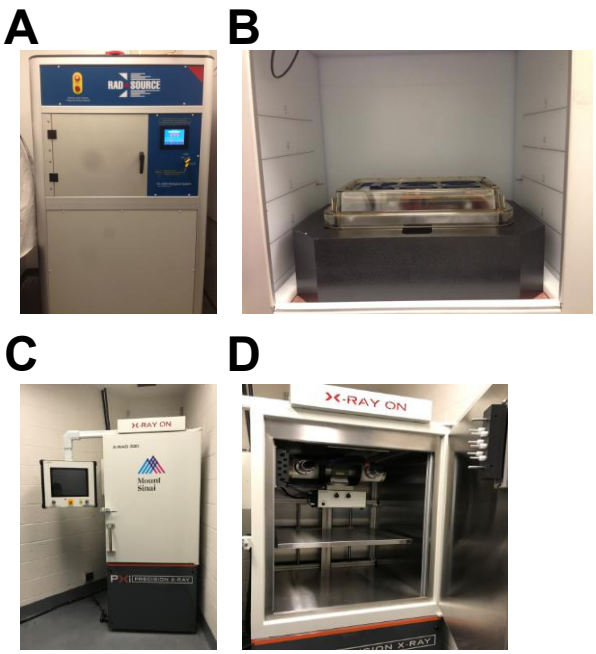

Figure 1. X-ray irradiators. **A.,** the RS 2000 Biological System X-ray Irradiator. **B.,** view of the RS 2000 irradiation chamber with reflector and mouse container at the bottom level; the marks on the walls of the irradiation chamber show the five height levels available. **C.,** the X-Rad 320 biological irradiator. **D.,** view of the X-Rad 320 irradiation chamber; the X-ray tube and the collimator combination is located on the adjustable top shelf.

Tissue processing and flow cytometry.

Processing of blood samples and flow cytometric analyses were conducted using standard protocols, reagents (including CD4, CD8, CD11b, CD45R/B220, CD45.1, CD45.2 and CD90.1 antibodies) and equipment as referenced or detailed in ref. (10).

Statistical analyses.

Data handling, analysis and graphic representation was performed using Prism 6.0c (GraphPad Software); statistical differences calculated by one-sample t-test or one-way ANOVA with Dunnett's multiple comparisons test.

RESULTS & DISCUSSION

We first generated sets of BM chimeras using CD45-congenic donors and recipients, irradiation with 2x600 cGy delivered with a RS2000 Biological System Irradiator (160 kV, 25 mA) identical to the instrument used by Gibson *et al.* (7), and i.v. transfer of 3-5x10^6 T cell-depleted BM cells (see Methods for further details). The composition of the peripheral blood compartment was analyzed six weeks later by flow cytometry using CD45.1- and CD45.2-specific antibodies to distinguish donor- and host-derived immune cells. Aiming for a reconstitution efficiency that reduced the contribution of host-derived leukocytes to <10%, we found that this irradiation protocol indeed allowed for population of the PBMC compartment with >94% donor-derived leukocytes; further stratification of these cells into lymphocytes and granulocytes as based on forward (FSC) and side-scatter (SSC) properties revealed particularly good results for granulocytes that contained <3% host-derived cells (***Fig.2A/B***). Similar results were obtained in another experimental cohort analyzed eight weeks after BM transfer that further showed

excellent reconstitution wit donor-derived CD11b^{+} myeloid cells (>97%) and B cells (>99%) (***Fig.2C/D***). Due to the greater radioresistance of host T cells and the delayed appearance of donor-derived T cell populations in the periphery (1), we waited for ten weeks after irradiation/BM transfer before conducting our T cell analyses. As shown in ***Fig.2E/F***, overall reconstitution remained excellent with >95% donor-derived peripheral blood lymphocytes but in the T cell compartment, ~16% of CD4^{+}T cells and up to 24% of CD8^{+}T cells were in fact of host origin. Prolonged observation of the same chimera cohort revealed no indications of compromised health, and T cell analyses conducted as late as 30 weeks after irradiation/BM transfer demonstrated a reduction of host-derived of CD4^{+}T cell frequencies to ~6% but no comparable decrease for host CD8^{+}T cells (not shown).

The “contamination” of the peripheral CD8^{+}T cell pool with host-derived cells poses a particular problem for studies that seek to harness the X-ray BM chimera approach for the specific study of CD8^{+}T cell immunity. Since higher energy photon radiation provides better penetration and dosage deposition at increased depth (4, 11), we sought to determine if an adjusted irradiation protocol would permit better CD8^{+}T cell reconstitution. We therefore conducted preliminary experiments using a higher energy X-ray source (X-Rad 320 Biological Irradiator, 320 kVp, 12.5 mA) and irradiated recipient mice with 2x500 cGy (we also used CD90.1-congenic donor BM in these experiments). T cell reconstitution assessed 6-8 weeks later showed a greater fraction of donor CD8^{+}T cells (83%) (***Fig.2G***) but 2/8 chimeras (25%) had to be euthanized, surviving mice exhibited ruffled furs, auricular necrosis, dry eyes and prolonged diarrhea, some failed to thrive and gain weight, and upon necropsy presented with signs of radiation enteritis (not shown). Nevertheless, due to additional experimental variables introduced in these experiments such as the use of stem cell-enriched BM cells we remain confident that suitable protocols for BM chimera generation will be developed that specifically make use of higher energy X-ray sources to improve the reconstitution with donor CD8^{+}T cells.

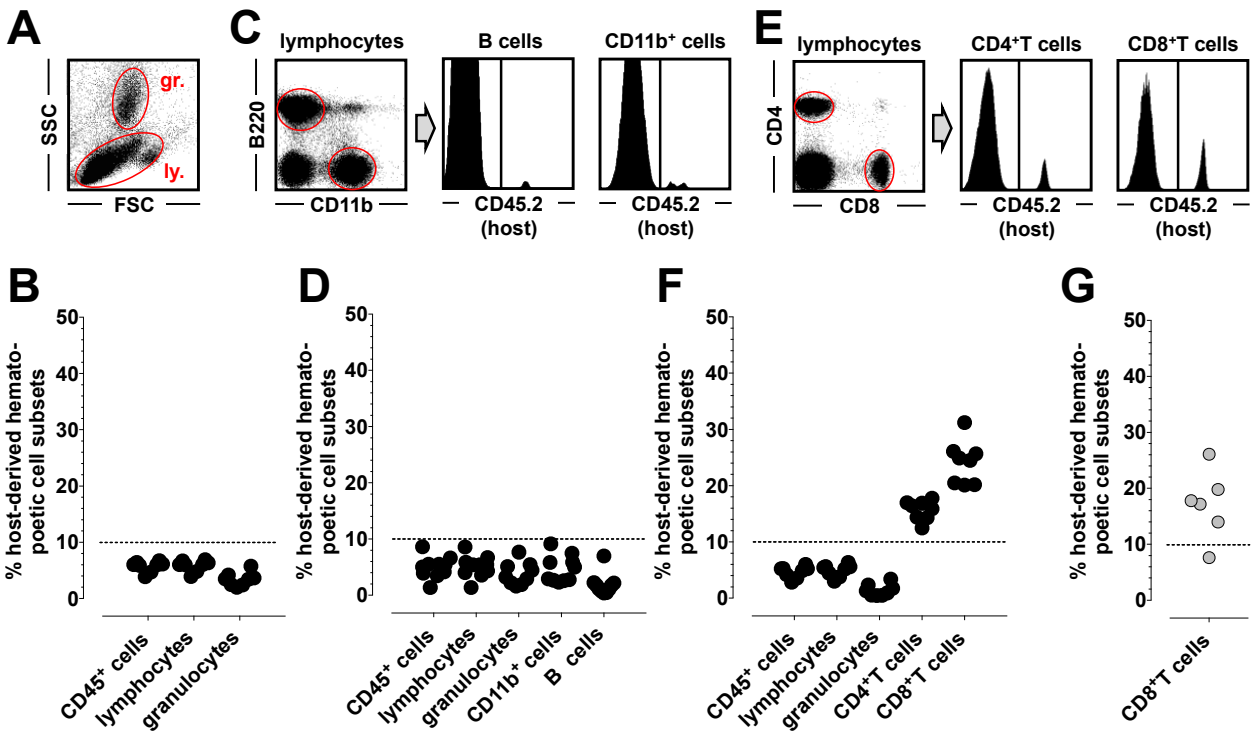

Figure 2. Reconstitution of the peripheral blood compartment in congenic BM chimeras. BM chimeras were generated using CD45- or CD90-congenic recipients and BM donors as well as various irradiation protocols as detailed in Methods. **A.,** differentiation of lymphocytes (ly.) and granulocytes (gr.) according to FSC/SSC properties in peripheral blood of a representative BM chimera (note that our blood processing protocols lead to partial loss of granulocytes such that their relative abundance among PBMC is reduced to ~5%). **B.,** relative proportions of host-derived leukocytes ($CD45^+$ cells), lymphocytes and granulocytes (see gating strategy in panel A); BM chimeras were generated using 2x600 cGy (old Hess Irradiator, details to be provided in Methods) and analyzed ~6 weeks after irradiation/BM transfer (n=8). **C. & D.,** analysis of a separate set of BM chimeras generated as in panel B and analyzed ~8 weeks after irradiation/BM transfer (n=10). The dot plot demonstrates identification of $B220^+$ B cells and $CD11b^+$ myeloid cells found within the lymphocyte gate; the representative histograms display the relative contribution of host-derived (here $CD45.2^+$) B and myeloid cells (note in particular the very low frequency of host-derived B cells). **E. & F.,** BM chimeras generated as in panel A and analyzed ~10 weeks later. Gating strategies for identification of $CD4^+$ and $CD8^+$T cells and their differentiation according to host origin ($CD45.2^+$) are shown (note especially the presence of ~24% host-derived $CD8^+$T cells). All host-derived $CD45^+$, lymphocyte, granulocyte, $CD11b^+$ myeloid and B cell populations quantified in panels B, D and F were found at frequencies significantly below 10% ($p<0.0001$ in one-sample t-tests). **G.,** BM chimeras were constructed using B6 ($CD90.2^+$) recipients and congenic ($CD90.1^+$) donors and an alternate irradiation protocol using a split dosage of 2x550 cGy (new Icahn irradiator, details to be provided in Methods). Analyses conducted ~7 weeks later (n=8) demonstrated a significantly reduced contribution of host-derived $CD8^+$T cells to the $CD8^+$T cell pool in comparison to $CD8^+$T cell data in panel F (~17%; $p= 0.0208$ using an unpaired t-test) but the BM chimeras also exhibited enhanced morbidity and mortality.

Altogether, X-ray irradiation at a dosage of 2x600 cGy using a 160 kV / 25 mA X-ray source allows for the generation and long-term survival of BM chimeras with an overall acceptable degree of chimerism for major immune cell populations (<10% of host-derived granulocyte, $CD11b^+$ myeloid, B cell and $CD4^+$T cell populations) but with the notable exception of $CD8^+$T cell compartment where only ~75% of cells were donor-derived. Although use of a higher energy source (320 kVp / 12.5 mA) resulted in improved reconstitution with donor-derived $CD8^+$T cells, associated adverse health effects limited the overall utility of the preliminary protocol employed. Thus, in regards to the specific study of $CD8^+$T cell populations there remains a need to develop optimized protocols that employ X-ray irradiation for the generation of BM chimeras.

REFERENCES

1. Spangrude GJ. Assessment of lymphocyte development in radiation bone marrow chimeras. *Curr Protoc Immunol.* 2008;Chapter 4(Unit 4 6.
2. Duran-Struuck R, and Dysko RC. Principles of bone marrow transplantation (BMT): providing optimal veterinary and husbandry care to irradiated mice in BMT studies. *J Am Assoc Lab Anim Sci.* 2009;48(1):11-22.
3. Dodd B, and Vetter RJ. Replacement of 137Cs irradiators with x-ray irradiators. *Health Phys.* 2009;96(2 Suppl):S27-30.
4. Yoshizumi T, Brady SL, Robbins ME, and Bourland JD. Specific issues in small animal dosimetry and irradiator calibration. *Int J Radiat Biol.* 2011;87(10):1001-10.
5. Potter CA, Longley SW, Scott BR, Lin Y, Wilder JA, Hutt JA, Padilla MT, and Gott KM. *SAND2013-0743: Radiobiological Studies Using Gamma and X Rays*. Sandia National Laboratories, Albuquerque, NM; 2013.
6. Dubé P. Considerations for rodent irradiation. https://www.taconic.com/taconic-insights/oncology-immuno-oncology/rodent-irradiation-considerations.html; 2017.
7. Gibson BW, Boles NC, Souroullas GP, Herron AJ, Fraley JK, Schwiebert RS, Sharp JJ, and Goodell MA. Comparison of Cesium-137 and X-ray Irradiators by Using Bone Marrow Transplant Reconstitution in C57BL/6J Mice. *Comp Med.* 2015;65(3):165-72.
8. Homann D, Dummer W, Wolfe T, Rodrigo E, Theofilopoulos AN, Oldstone MB, and von Herrath MG. Lack of intrinsic ctla-4 expression has minimal effect on regulation of antiviral T-cell immunity. *J Virol.* 2006;80(1):270-80.
9. Neudecker V, Brodsky KS, Clambey ET, Schmidt EP, Packard TA, Davenport B, Standiford TJ, Weng T, Fletcher AA, Barthel L, et al. Neutrophil transfer of miR-223 to lung epithelial cells dampens acute lung injury in mice. *Sci Transl Med.* 2017;9(408).
10. Eberlein J, Davenport B, Nguyen TT, Victorino F, Karimpour-Fard A, Hunter LE, Clambey ET, Kedl RM, and Homann D. Aging promotes acquisition of naïve-like CD8+ memory T cell traits and enhanced functionalities. *J Clin Invest.* 2016;106(10):3942-60.
11. Belley MD, Ashcraft KA, Lee CT, Cornwall-Brady MR, Chen JJ, Gunasingha R, Burkhart M, Dewhirst M, Yoshizumi TT, and Down JD. Microdosimetric and Biological Effects of Photon Irradiation at Different Energies in Bone Marrow. *Radiat Res.* 2015;184(4):378-91.

Comparative analysis of X-ray vs ^{137}Cs radiation in zebrafish embryos: cell death, organismal radiosensitivity and p53-dependence

Renuka Raman, Yuanyuan Li and Samuel Sidi
Department of Hematology/Medical Oncology
Icahn School of Medicine at Mount Sinai

INTRODUCTION

Our laboratory uses zebrafish embryos as a model to recapitulate prevalent mechanisms of tumor resistance to radiation therapy (R-RT) in vivo. One such mechanism of tumor R-RT is mutational inactivation of the p53 transcription factor, which occurs in ~50% of solid tumors[1]. Cancer cells with mutant p53 fail to trigger apoptotic or senescence gene-expression programs in response to ionizing radiation (IR)-induced double-strand DNA breaks (DSBs)[2].

Zebrafish faithfully recapitulate mammalian apoptotic signaling, develop rapidly in vitro, lay eggs in large numbers, and the effects of radiation exposure are easy to assess in embryos without parental killing. Keeping these advantages in mind, in the past, we have used zebrafish to identify the PIDDosome pathway as a means to induce an apoptotic response to ionizing radiation in otherwise radioresistant p53 mutant embryos[3]. Our lab developed a whole-animal zebrafish model of mutant TP53-driven R-RT for use in unbiased genetic and chemical screens to screen for novel radiosensitizing agents. In this model, zebrafish embryos homozygous for the M214K (MK) mutation in p53 display fully penetrant R-RT, as evidenced by a complete lack of cell death induction in response to IR and a complete lack of IR-induced dorsal tail curvatures (DTC)[3].

Because the institution is transitioning from Cs irradiation to an X-ray irradiator we performed a series of experiments comparing various doses of X-irradiation to our standard Cs irradiation to identify conditions best suited for further use of the zebrafish model to screen for novel radiosensitizers. We used our recently identified novel radiosensitizer oxfendazole as a positive control to standardize conditions using the X-ray irradiator for future use. In addition to the dose of X-ray radiation, the developmental stage of embryos, type of filter, stationary/rotating position of the sample turntable and the optimum distance of the sample from the source of radiation were also standardized. At the end of each experiment, the extent of apoptosis achieved after X-ray treatment and the number of embryos exhibiting radiosensitization- displayed by either curved or bowed embryos- was analyzed on the 5th day post radiation.

MATERIALS AND METHODS

Zebrafish maintenance

Adult zebrafish were maintained at 28^{o}C on a 14:10 hour light:dark cycle. Embryos of p53$^{MK/MK}$ fish and wild-type zebrafish from the AB line were used. All experiments were conducted in accordance with the policies of the Mount Sinai Institutional Animal Care and Use Committee.

Zebrafish X-ray irradiation and drug treatments

Zebrafish embryos were collected and washed using standard zebrafish E3 culture medium (5 mmol/L sodium chloride (NaCl), 0.33 mmol/L calcium chloride, 0.33 mmol/L magnesium sulfate heptahydrate, 0.17 mmol/L potassium chloride (KCl)) at the one-cell to two-cell stage. Live embryos were dechorionated in pronase (2.0 mg/mL in egg water) for 7 minutes and rinsed three times in egg water at 17 hpf, 19hpf or 23hpf. For each experiment, a minimum of 15 wild-type and p53$^{MK/MK}$ embryos were arranged into each well of a 24-well plate. For experiments involving drug treatments, oxfendazole was used at a final concentration of 20µg/ml. Each well contained 500µl of E3 medium in presence of absence of drug. Plates containing embryos were γ-irradiated at different developmental time points (18hpf, 20hpf or 24hpf) using an X-ray irradiator (X-RAD 320 PRECISION X-RAY) at different doses depending upon the experiment. Embryos treated with the ^{137}Cs-irradiator at 1500 Rads/15 Grays were used as positive control. After irradiation, the embryos were returned to the 28 ^{o}C incubator. Embryos were washed three times 6 hours post IR treatment (hpIR), and scored grossly for neural opacity and stained with acridine orange (AO) dye. Embryos were washed post AO imaging and were rinsed with 19.7 mmol/L 1-phenyl-2-thiourea (Sigma, St Louis, Missouri, USA) water to prevent pigment formation before 30hpf. Embryos were rescored at 72 hpf and 120 hpf for curved tails and gross morphological changes. Pictures were obtained of tricaine-anesthetized embryos mounted on 2-3% methylcellulose and imaged with a Nikon SMZ 1500 fluorescence microscope.

Acridine Orange (AO) Labeling.

Cell apoptosis in living embryos was detected through staining with the vital dye acridine orange (AO) 6 hours post radiation treatment. Embryos from all groups were washed with E3 three times, then incubated in 1 mL of AO solution (5 µg/mL in E3) for 20 minutes in the dark at 28 °C. The embryos were washed three times with E3 thoroughly, followed by anaesthetization using 0.01% MS 222 (Sigma). Image of each embryo were captured under a Nikon SMZ 1500 fluorescence microscope and the fluorescence of apoptotic signals was measured and quantified using ImageJ.

Statistics

Data in bar graphs are represented as mean ± SD and plotted in EXCEL.

RESULTS AND DISCUSSION

We observed that although increasing doses of X-ray treatment (5, 8 and 10 Gray), lead to an increase in cell death as observed using AO staining, a significant fraction of wild type or p53 mutant embryos displaying bent tail phenotypes at 5 days post fertilization was not observed (Fig. 1, 2). Majority of wild type embryos treated with 12.5 and 15 Gray X-ray radiation displayed radiosensitization and exhibited a bowed (tail down) phenotype as opposed to Cesium IR treated embryos, which display radiosensitization in the form of curved (tail up) phenotype (Fig. 1,2). This difference in radiosensitization phenotype between X-ray and Cesium IR can be attributed to the qualitative differences between the two kinds of radiation and the biological response elicited in the zebrafish embryos. We observed that Filter 2 (which filters non-specific low dose ionizing radiation) showed lower toxicity and cleaner phenotypes as compared to Filter1. 12.5 Gray X-ray treatment led to a developmental stage dependent radiosensization phenotype. Maximum radiosensitization using **12.5 Gray X-ray was observed in 24hpf wild-type embryos** (75-80%), which exhibited bowed tail phenotype, while *p53* mutant embryos displayed minimal radiosensitization (less than 5%), which is ideal for screening novel radiosensitizers in the *p53* mutant background. 15 Gray X-ray treatment caused radiosensitization in both wild type embryos (bowed phenotype) and p53 mutants (curved phenotype). Radiosensitization in p53 mutant embryos after oxfendazole treatment comparable to Cesium IR was seen in 12.5 Gray X-ray treated 24 hpf embryos when the turntable –on which plates containing embryos is placed- is kept stationary at a distance of 50 cm from the X-ray source (Fig. 4), as opposed to rotating, in which case radiosensitization was not observed (Fig.3). In conclusion, 12.5 Gray X-ray radiation dose, when administered to 24hpf zebrafish embryos kept on a stationary turntable at a distance of 50cm from the X-ray source can be used to screen for novel radiosensitizers.

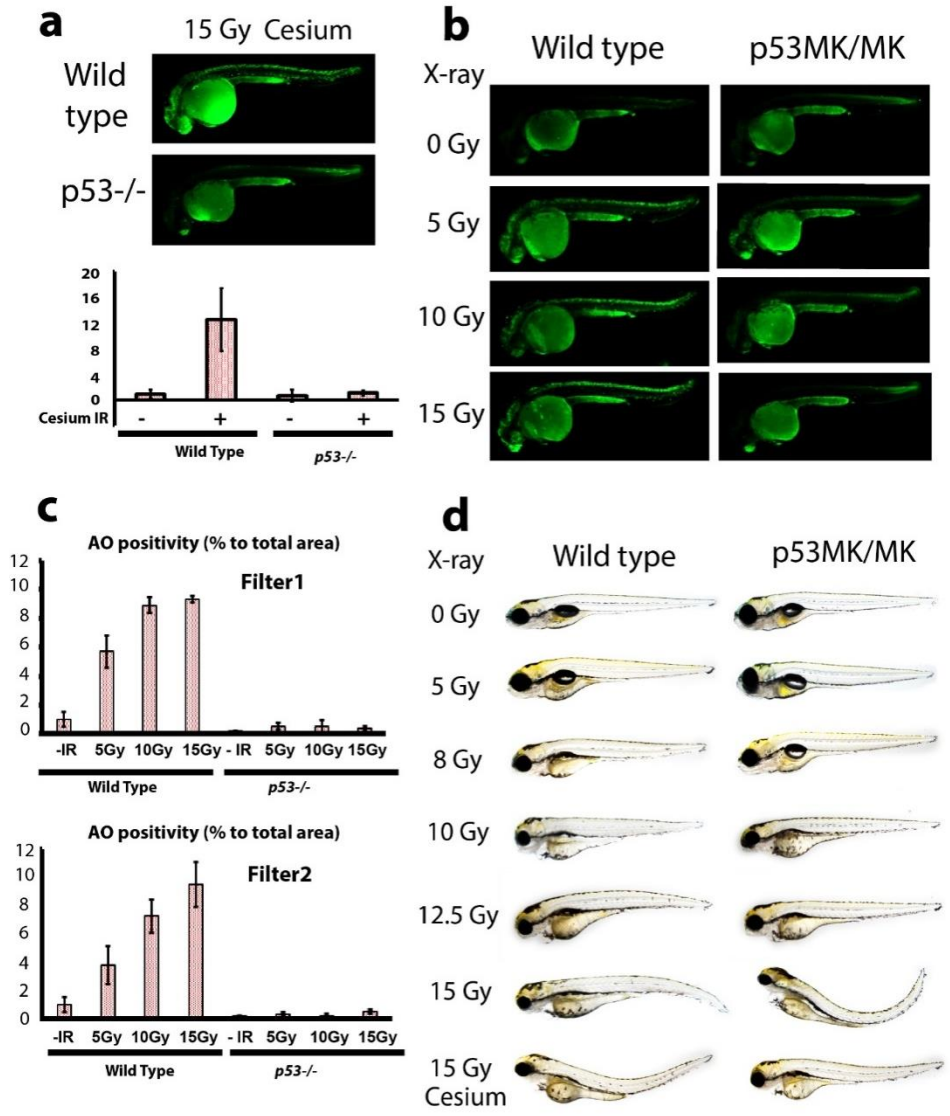

Figure1 (a) Wild type (WT) and *p53*$^{MK/MK}$ (p53 mutant) zebrafish embryos treated at 18 hours post fertilization (hpf) with γIR, gamma-irradiation from ^{137}Cs source (15 Gy). Embryos were stained with Acridine Orange (AO) at 6 hpIR to estimate cell death. Note the strong AO staining in wild type embryos and a complete absence of AO labeling in the brain and spinal cord of the irradiated p53 mutant. AO uptake by cells was quantified in live embryos at 7.5 hpIR. **(b)** Zebrafish embryos treated at similar stage (18hpf) with X-ray irradiation (5, 10 or 15G) using Filter1 or Filter2 stained with the cell death marker acridine orange (AO) 6 hpIR. Similar to Cesium γIR source, the stripe of AO+ cells is seen in radiation sensitized WT embryos, but not in p53 mutant embryos. **(c)** AO staining intensity increases with increasing dose of X-ray irradiation (5, 10 and 15G) using Filter1 and Filter2. **(d)** Representative phenotypes displayed by WT and *p53*$^{MK/MK}$ zebrafish embryos at 5 day post fertilization (dpf), post X–ray treatment at doses of 5G, 8G, 10G, 12.5G or 15G at 18hpf. X-ray treatment at doses of 5G, 8G or 10G at 18hpf did not have any morphological effect either on WT or p53 mutant embryos. X-ray treatment at 12.5G and 15G, gave rise to mainly three categories of morphological phenotypes namely straight (normal), bowed tail (tail down) and curved tail (tail up) phenotype. Experiments were repeated at least twice using a minimum of 15 embryos of each genotype for the analysis.

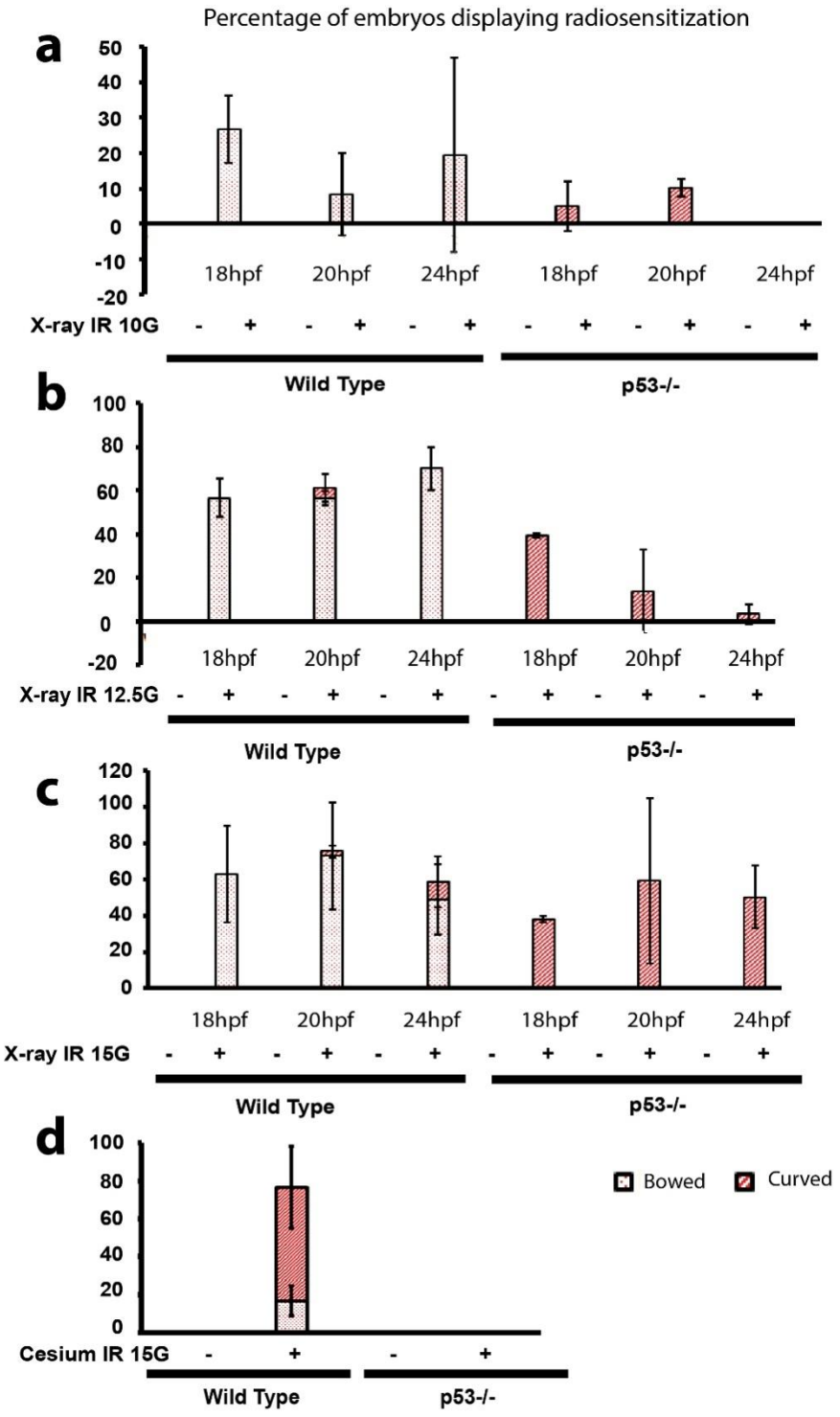

Figure2 Comparison of 5 day phenotype post X-ray treatment at 10G **(a)**, 12.5 G **(b)** and 15G **(c)** respectively at different time points (18, 20 and 24hpf) in wild type and *p53*$^{MK/MK}$ embryos. The Cesium IR radiation (15G) at 18hpf is used as a positive control for irradiation **(d)**. Experiments were repeated at least twice using a minimum of 15 embryos of each genotype for the analysis.

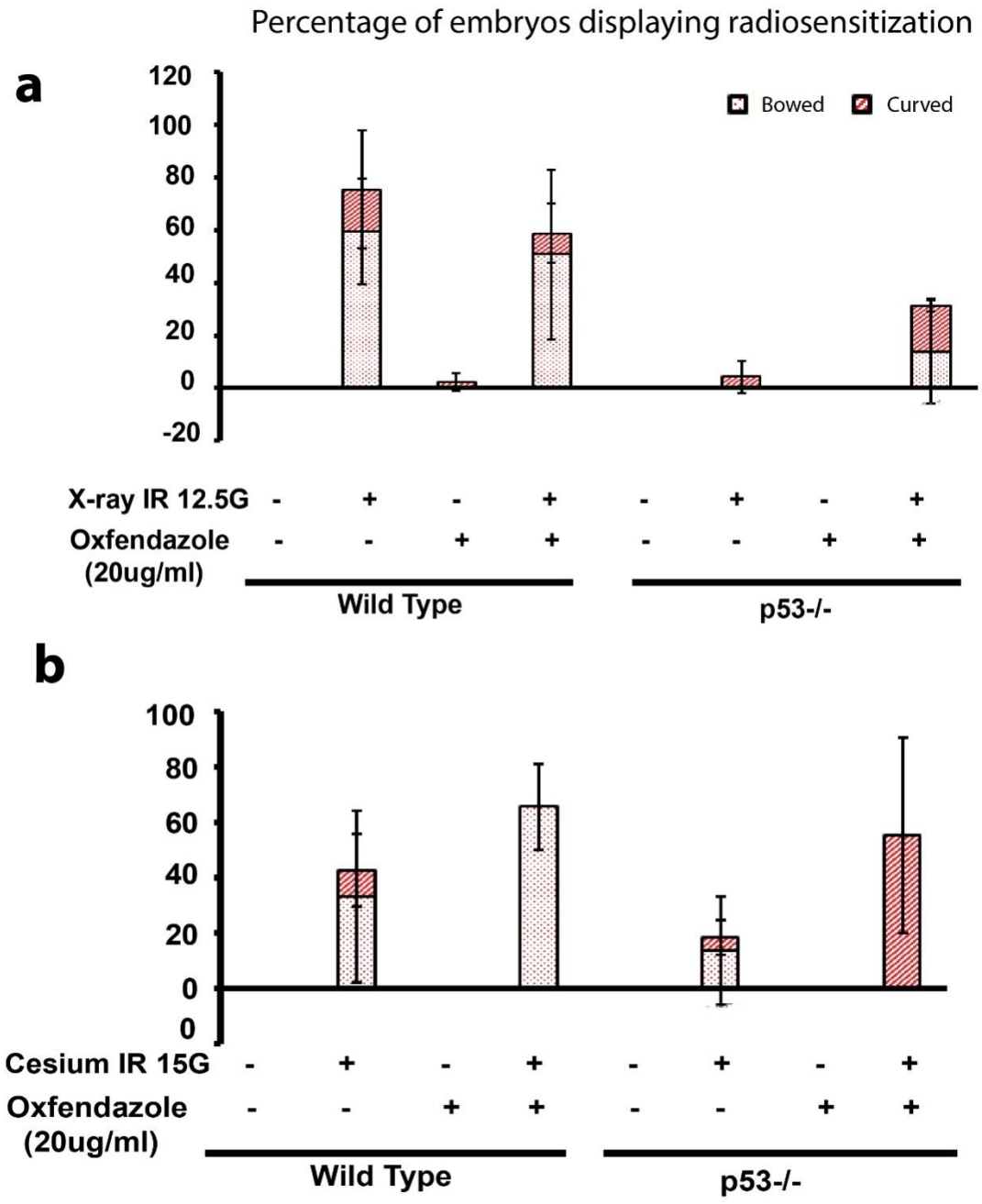

Figure 3 (a) Comparison of 5 day phenotype between X-ray and Cesium IR irradiation after oxfendazole treatment in wild type and $p53^{MK/MK}$ embryos post treatment. X-ray treatment (12.5G) was given at 24hpf, while the Cesium IR radiation (15G) was administered at 18hpf. Embryos were treated 1 hour prior to IR treatment with oxfendazole (20ug/ml). Percentage of embryos displaying bowed (tail down) or curved (tail up) phenotype have been plotted on the Y axis.

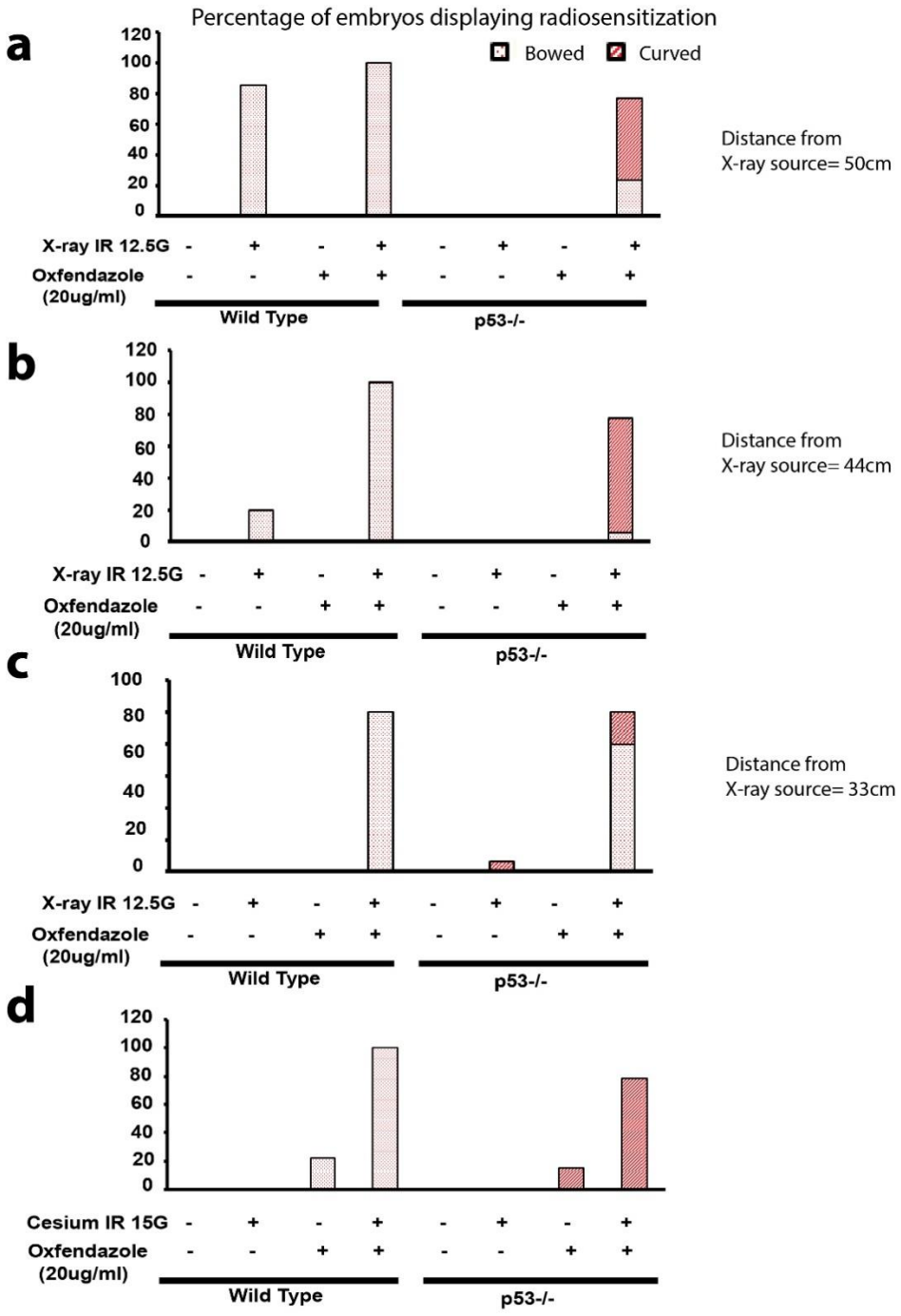

Figure 4 Comparison of 5 day phenotype between wild type and $p53^{MK/MK}$ embryos exposed at 24hpf to 12.5G X-rays, irradiated at different distances **(a,b,c)** from X-ray source after oxfendazole treatment. 18hpf embryos treated with oxfendazole and Cesium IR were used as control **(d)**. Percentage of embryos displaying radiosensitization phenotypes namely-bowed (tail down) or curved (tail up) phenotype have been plotted on the Y axis. The experiment was performed using a minimum of 15 embryos of each genotype.

REFERENCES

1. Poeta, M. L. *et al.* TP53 mutations and survival in squamous-cell carcinoma of the head and neck. *N. Engl. J. Med.* **357,** 2552–2561 (2007).

2. Johnstone, R. W., Ruefli, A. A. & Lowe, S. W. Apoptosis: a link between cancer genetics and chemotherapy. *Cell* **108,** 153–164 (2002).

3. Sidi, S. *et al.* Chk1 suppresses a caspase-2 apoptotic response to DNA damage that bypasses p53, Bcl-2, and caspase-3. *Cell* **133,** 864–877 (2008).

Comparison of effect of X-ray and Cs irradiation on PBMC in vitro

Naoko Imai, Sacha Gnjatic

Department of Medicine, Hematology & Oncology, Icahn School of Medicine at Mount Sinai

Introduction

Our laboratory assesses humoral and cellular responses for cancer antigens (cancer-testis antigens, viral antigens, neoantigens, etc.) to develop more effective cancer immunotherapies. Because precursor frequency of cancer antigen-specific T cells in circulation is usually very low, it is difficult to detect these cells *ex vivo* from peripheral blood mononuclear cells (PBMC). Thus, our regular protocol to assess CD8/CD4 T cell responses against cancer antigens includes an *in vitro* sensitization to expand and help detect antigen-specific T cell responses by ELISPOT, cytokine ELISA, and/or ICS[1)]. To presensitize CD8/CD4 T cells, we stimulate positively-selected CD8/CD4 T cells from PBMC with peptide-pulsed antigen-presenting cells (APC) for 10-20 days. As APC, we use cells from the $CD4^{-}CD8^{-}$ fraction of PBMCs that include mainly B cells, monocytes, and granulocytes. APCs are pulsed with antigen for overnight, irradiated, and then co-cultured with CD8/CD4 T cells. The irradiation inhibits APCs from proliferating but allows the cells to survive a few hours to several days to allow them to present antigen to T cells. Irradiation also prevents contamination of cultures from outgrowth of T cell lymphocytes potentially still remaining in the $CD4^{-}CD8^{-}$ fraction of PBMCs. We have used a Cesium (Cs)-based instrument to irradiate APCs for many years, but institutional policies required us to switch over to an X-ray irradiator and convert our irradiation protocol from a risky radioactive source to safer X-rays, following recommendations from the National Academy of Science. Only a few reports have compared the effect of irradiation by X-rays versus gamma-rays on red blood cells[2,3,4] and they conclude that X- and gamma-ray irradiation can be regarded as equivalent. However, there is no literature that shows such comparison on PBMCs, so we decided to benchmark the new X-ray irradiator to our old Cesium-based one for this purpose. Another issue was to test the method of irradiation with X-rays, where only plates and dishes were recommended by the manufacturer even though our protocol calls for use of cryotubes, 15 ml or 50 ml tubes. To optimize the novel X-ray irradiation protocol for PBMC and match results from our previous Cs-based conditions, we measured the viability of lymphocytes and myeloid cells over time after various doses of X-ray irradiation and used various cell containers to compare with our current standard Cs-irradiator condition (30 Grey(Gy), cryotube).

MATERIALS & METHODS

1. Cell preparation. The protocol was based on our regular standard operating procedures for T cell presensitization as previously described[1], with modifications. We used whole PBMC instead of $CD4^{-}CD8^{-}$ fraction to simplify measurements. Cryopreserved PBMCs from two healthy donors were thawed, washed with X-VIVO15 medium (LONZA) and rested for 2h in a CO_2 incubator at 37°C. Cells were resuspended at a concentration of $6x10^6$/ml in X-VIVO15 and

split equally to 6 different irradiation conditions ($3x10^6$/0.5ml, each) as indicated in Table 1. Cells were then washed and resuspended in RPMI medium 1640 (Gibco) with 10% human AB serum (GEMINI), GlutaMAX-I (2 mM, Gibco) and Penicillin-Streptomycin (100 U/ml, Gibco) and seeded into round-bottomed 96-well plates (Corning) at a concentration of $1x10^6$ cells per well. After 20 hours, IL-2 (10 U/ml, Roche) and IL-7 (20 ng/ml, R&D Systems) were added. Subsequently, one-half of the medium was replaced by fresh complete medium containing IL-2 (20 U/ml) and IL-7 (40 ng/ ml) twice a week.

2. Comparison Groups. Results were compared in the 3 following groups. A) Irradiator: Cs and X-ray, B) Container: Cryotube, 50ml tube and 24 well plate, and C) Dose: 25Gy, 30Gy and 35Gy, as shown in Table 1 and Figure 1.

3. Flow Cytometry. On day 1, 5, and 9, cells were stained with eBioscience™ Fixable Viability Dye eFluor™ 520 (Invitrogen), acquired on a BD FACSCalibur (BD Biosciences) and analyzed by FlowJo (TreeStar). Lymphocytes and myeloid cells were determined by FSC/SSC plot as shown in Figure 2. When cells were collected from the 96-well plate on day 5 and 9 for flow cytemetry analysis, 8% and 20% of the volume of cell suspension per well was collected, respectively. After staining with viability dye, all cells were acquired and counted by BD FACSCalibur. The viable cell number per well was calculated using the portion of used, the acquired number of cells by FACSCalibur and the percentage of viability.

4. Statistical Analysis. Statistical analyses were performed using Prism (GraphPad Software). Change of percentage of viable cells was compared by multiple *t* test. A p-value <0.05 was considered significant. Error bars displayed are the mean with SD. Regression analysis was also performed to compare Cs and X-ray irradiator.

Results and discussion

As shown in Figure 3A, both the number of viable cells per well and the percentage of viable lymphocytes and myeloid cells was very similar at day 1, 5 and 9 following irradiation of cells in cryotubes at 30Gy with either the X-ray or gamma-ray irradiator. As expected, the number of viable cells and the percentage of viable lymphocytes and myeloid cells decreased in a time dependent manner. In addition, there was no significant differences in viable cell number and dynamic viability percentage observed based on the type of container used for irradiation (Figure 3B). Finally, numbers of total viable cells and percentages of cell subset viability over time observed at 25Gy, 30Gy and 35Gy showed no significant differences (Figure 3C).

Overall, we observed very similar trends in changes of percentage of viable lymphocytes and myeloid cells in all comparison groups: A) Irradiator, B) Container and C) Dose (Figure 3), and those from Cs and X-ray irradiators were well correlated (Figure 4), indicating that any of these conditions were sufficient to inhibit APC proliferation.

In conclusion, 30Gy irradiation by X-ray irradiator is equivalent to the 30Gy irradiation by gamma-ray of Cesium, which is our current standard. Moreover, various types of container, including cryotubes, 50ml tubes, or plates can be used for X-ray irradiator with similar efficacy.

We therefore have now switched from Cs to X-ray irradiator for our laboratory and can recommend X-ray irradiation when required in cell cultures with human lymphocytes.

Units depended on irradiator, container and irradiated dose and comparison groups.

Irradiation condition	Irradiator	Container	Dose	Comparison Group		
				A) Irradiator	B) Container	C) Dose
1	Cs	2.0 ml cryotube	30 Gy	✓		
2	X-ray	2.0 ml cryotube	30 Gy	✓	✓	✓
3		50 ml tube	30 Gy		✓	
4		24-well plate	30 Gy		✓	
5		2.0 ml cryotube	25 Gy			✓
6		2.0 ml cryotube	35 Gy			✓

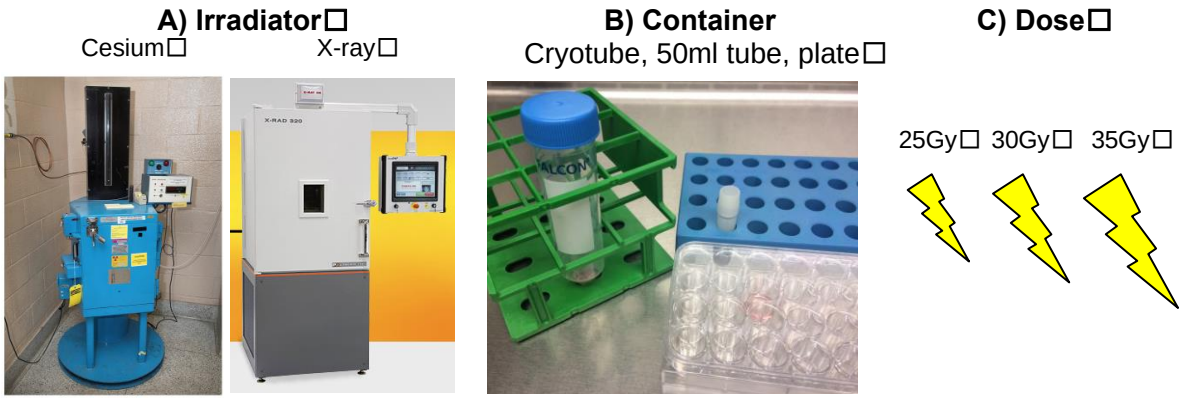

Figure 1. Illustrated comparison groups.

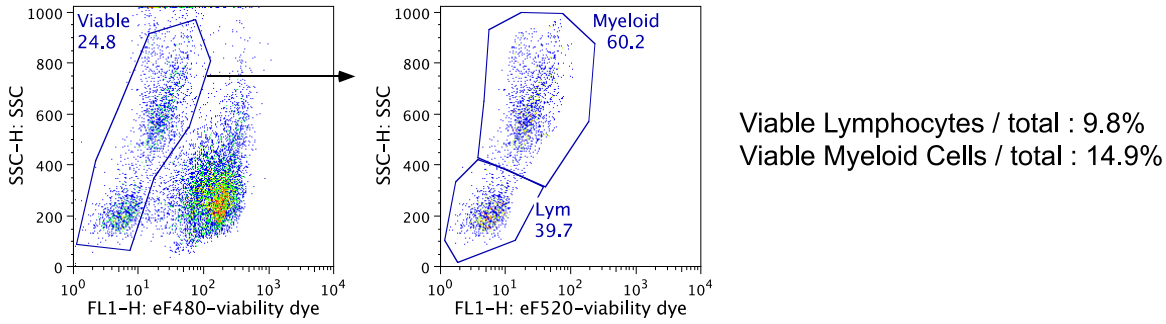

Figure 2. Gating strategy. Viable lymphocytes and myeloid cells were determined by FSC/SSC plot and viability dye.

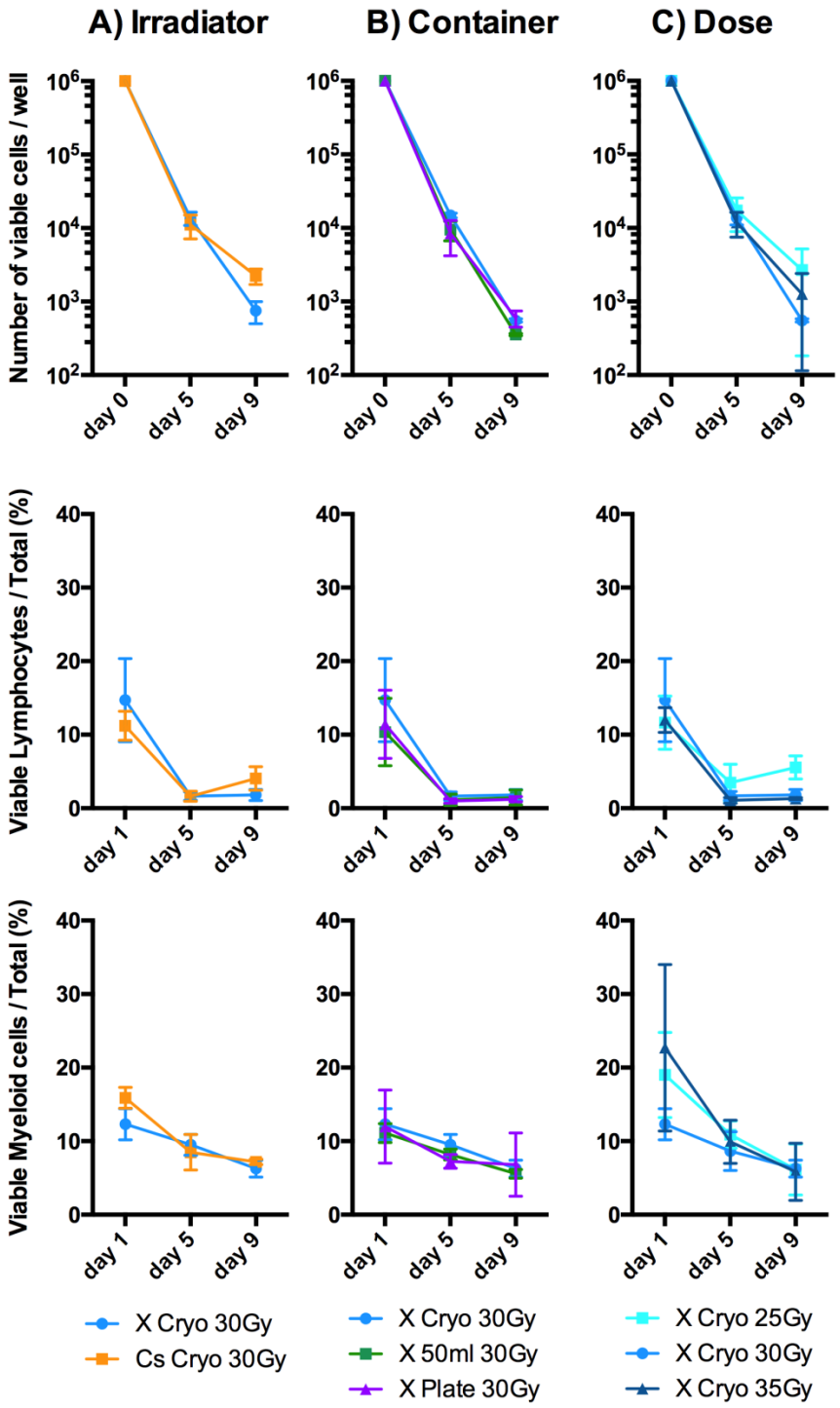

Figure 3. Change of percentage of viable cells. Upper panel and lower panel show percentage of viable lymphocytes and myeloid cells in total cells, respectively. X = X-ray irradiation; Cs = Cesium irradiation; Cryo: 2.0 ml cryotube; 50ml: 50 ml tube; Plate: 24-well plate; Gy: Gray.

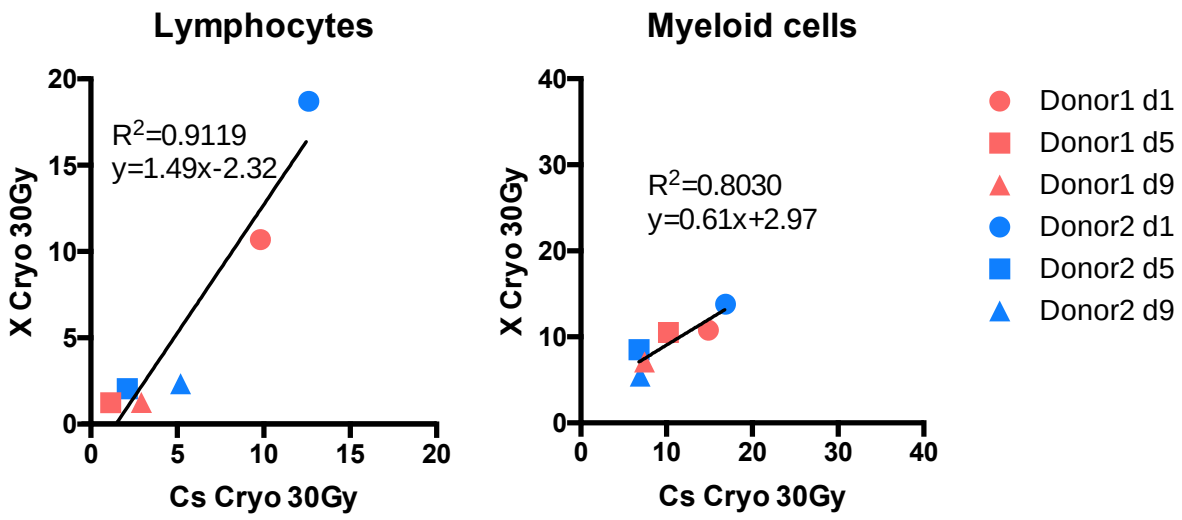

Figure 4 Comparison of percentage of viable lymphocytes and myeloid cells in total cells between Cs and X-ray irradiator. Line with linear regression was fitted to each graph. d: day after irradiation.

References

1. Atanackovic, D. *et al.* Monitoring CD4+ T cell responses against viral and tumor antigens using T cells as novel target APC. *J Immunol Methods* **278,** 57–66 (2003).
2. Dodd, B. & Vetter, R. J. Replacement of ^{137}Cs irradiators with x-ray irradiators. *Health Phys* **96,** S27–30 (2009).
3. Janatpour, K. *et al.* Comparison of X-ray vs. gamma irradiation of CPDA-1 red cells. *Vox Sang.* **89,** 215–219 (2005).
4. MacLellan S. X-irradiation as an alternative to gamma-irradiation. Change Notification UK National Blood Services No. 6 - 2009. Available from https://www.transfusionguidelines.org/document-library/documents/change-notification-no-6-2009

Comparison of X-ray vs Cs-137 irradiation for producing mitotically-inactivated mouse embryonic fibroblasts to grow mouse embryonic stem (ES) cells.

Nika Hines, Pedro Sanabria and Kevin Kelley

Irradiator CoRE Facility
Director, Kevin Kelley, Ph.D.
Icahn School of Medicine at Mount Sinai
New York, NY 10029

Introduction

The Irradiator CoRE Facility has operated a Cs-137 irradiator (Model 6810, J.L. Shepherd and Associates) from 2008 until January of 2018, and an X-RAD 320 (320 kV, Precision X-Ray, Inc.) since January, 2017. The goal of this facility is to irradiate biological samples (cell lines or mice) for Mount Sinai PIs and their staff. To meet this goal, and enhanced security measures surrounding the Cs-137 irradiator, the CoRE Facility has trained dedicated staff who operate the Cs-137 and X-ray irradiators. Due to increasing security concerns, the X-RAD 320 was purchased so that the Cs-137 machine could eventually be removed from the CoRE Facility. From March 2017 until the removal of the Cs-137 machine in January 2018, the facility staff assisted various PIs with comparative studies between the Cs-137 and X-ray machines, to determine parameters under which the X-ray machine would give comparable results to those obtained with the Cs-137 irradiatior.

One of the users of the Irradiator CoRE is the Mouse Genetics and Gene Targeting (MGGT) Core facility, which is also directed by Dr. Kelley. The MGGT CoRE performed comparative studies on the mitotic inactivation of mouse embryonic fibroblasts (MEFs). MEFs are required for the growth and maintenance of the pluripotent state of mouse embryonic stem (ES) cells. These MEFs are used as a feeder layer upon which mouse ES cells grow, providing growth support for the ES cells and keeping them in a de-differentiated (pluripotent) state. In order to keep the MEFs from outgrowing the ES cells in these co-cultures, they must be mitotically inactivated by irradiation or mitocmycin-C treatment so that they do not continue to divide, but continue to produce the necessary factors required by ES cells. The MGGT CoRE uses irradiation to prepare the MEFs, and did a comparative anaylsis of MEFS prepared by either Cs-137 or X-ray irradiation. The results of this comparative study will be presented and discussed below.

Materials and Methods

1. **Preparation of mouse embryonic fibroblasts**. Since many commonly used mouse ES cells are resistant to treatment with neomycin (G418 resistance; $G418^r$) due to the selectable marker used in gene targeting, mouse embryos from a $G418^r$ line were generated by timed matings of homozygous males and females of a Thy-1.2 knockout line that carries a neomycin resistance gene. Embryos were isolated at embryonic day 14.5 (E14.5), rinsed twice in phosphate buffered saline (PBS), and used to generate MEFs. Briefly, tissue from the E14.5 embryos was treated with 0.05% trysin/0.53M EDTA (trypsin/EDTA) until a uniform suspension of cells was achieved. These cells were then plated into 150 mm tissue culture dishes (the equivalent of cells from 1 embryo per dish) using Dulbecco's Modified

Eagle Medium (DMEM) supplemented with 10% fetal calf serum (FCS) and penicillin/streptomycin. When confluent, the MEFs were treated with trypsin/EDTA, centrifuged at 1500 RPM for 5 minutes to pellet the cells, and then resuspended in DMEM freezing media to a final concentration of 15% FCS and 10% dimethylsulfoxide (DMSO). Two cryovials per 150 mm dish were prepared, frozen slowly at -80^{o}C overnight, and then transferred to a liquid nitrogen freezer for long-term storage.

2. **Irradiation of mouse embryonic fibroblasts**. To prepare irradiated MEFs, one vial of cryopreserved MEFs was thawed and plated into three 150 mm dishes. These three dishes were split 1:3 once they reached confluence (in 2-3 days), and then split 1:3 one more time after the second set of dishes reached confluence, to generate a total of twenty seven 150 mm dishes of MEFs.

When the 27 dishes were confluent, the MEFs were removed from the dishes by treatment with trypsin/EDTA, centrifuged at 1500 RPM for 5 minutes to pellet the cells, and then resuspended in a final volume of 54 ml of DMEM, 10% FCS. One 50 ml sealed tube containing 45 ml of this cell suspension was irradiated with 3,000 Rads (30 Gy) in the Cs-137 irradiator, and one 15 ml sealed tube containing the remaining 9 ml of cell suspension was irradiated with 3,000 Rads (30 Gy) in the X-Rad 320 machine. Equal volumes of a 2x freezing media (DMEM with 30% FCS and 20% DMSO) were added to each tube after irradiation, and 1 ml aliquots were cryopreserved in cryovials by slow rate freezing at -80^{o}C overnight, followed by transfer to a liquid nitrogen freezer for long-term storage. This experiment generated 90 vials of cryopreserved MEFS that were mitotically-inactivated by Cs137 irradiation, and 18 vials of cryopreserved MEFS that were mitotically-inactivated by X-ray irradiation.

3. **Comparison of Cs-137 and X-ray irradiated mouse embryonic fibroblasts**. To compare the efficiency of mitotic inactivation using the different sources of radiation, one vial of cryopreserved MEF stock from Cs-137 or X-ray irradiation was thawed, and serial dilutions of 1:2, 1:4, 1:8, 1:16, 1:32 and 1:64 were plated into individual wells of a 24 well plate (with each well of the 24 well plate having a surface area of 2 cm^2). The cells were observed the day after plating to determine how well the MEFS had survived each type of irradiation, and they were also observed for an additional 5 days to confirm that the cells were indeed mitotically-inactive (growth-inhibited).

Results and Discussion

A comparison was conducted between MEFs irradiated by a Cs-137 source and an X-ray source. As described in Materials and Methods, after irradiation and cryopreservation, MEFS irradiated by the two different methods were thawed and serially diluted in side-by-side comparisons. For the purposes of calculation, the area covered by confluent MEFs in a 150 mm dish is 156.25 cm^2, so the 27 dishes that were used to generate the MEFs for this comparative study have a total surface area covered by cells of 4,218.75 cm^2. After irradiation, 108 vials of cryopreserved cells were prepared, which means that each vial would contain 4,218.75 cm^2/108 vial, or approximately 39 cm^2/vial. This is assuming a theoretical efficiency of 100% at each step of the preparation of the irradiated MEFS (isolation, irradiation, freezing and thawing). In reality, the efficiency is closer to 50-75%, as there are always losses at each step, especially after freezing and thawing of the cells. After plating the serial dilutions mentioned above, the irradiated MEFs from both machines were carefully monitored for 5 days, to yield two crucial

observations. The first is that the dilution at which each irradiated MEF type was confluent was found to be somewhere between the 1:8 and 1:16 dilution (assumed to be midway at 1:12) for both samples, suggesting that each sample contained approximately 24 cm^2 of cells per cryopreserved vial (the dilution factor of 12 multiplied by 2 cm^2 per well). There was no difference observed between the survival of MEFs irradiated by Cs-137 or X-ray. Other than the machine used to irradiate the cells, these MEFs were treated identically in a side-by-side comparison, so the only variable between them is the source of irradiation. The second observation was that the MEFs treated by both types of irradiation were clearly mitotically-inactivated, as there was no continued growth in any of the serially diluted wells. This would have been readily apparent, as cells that were not mitotically inactive would have continued to grow, resulting in wells becoming confluent at higher dilutions with the passage of time. The result of this comparison is that there were no quantitative or qualitative differences observed between MEFs irradiated by Cs-137 or X-ray at 3,000 Rads (30 Gy) in either machine. This observation of no significant difference in the irradiation of cells in either the Cs-137 or X-ray machines was observed by a number of other PIs during the period in which comparative studies were conducted between the two machines.

X-Ray Irradiation Is the Preferred Method of Irradiation for Tumor Cell Immunization

Ananda Mookerjee and Thomas Weber

Cardiovascular Research Center

Department of Medicine/Cardiology

Icahn School of Medicine at Mount Sinai

Introduction :

We are working on immunotherapy of ovarian cancer. Ovarian cancer is a major killer and is often detected late as it progresses without much symptom. We are currently testing vaccination with tumor cells transfected with genes that can introduce neo-antigens. We have already tested this vaccination in a prophylactic model of ovarian cancer and obtained promising results. Based on these encouraging data, we plan to proceed to therapeutic immunization.

Our vaccination strategy is to introduce specific genes by transient transfection to stimulate tumor cells to synthesize neo-antigens. 48 hours after transfection, we then lethally irradiate these cells and use them to immunize animals. In the prophylactic model, following 2 immunizations, the animals are challenged with live tumor cells. The neoantigens presented on the irradiated tumor cells trigger an immune response and due to epitope spreading these immune cells can also target untransfected live tumor cells. In therapeutic model, the animals will be vaccinated 7 days post tumor inoculation and will be boosted by another vaccine. We then perform a variety of experiments to test different immunological parameters that include ELISA, Flow cytometry, Immuoprecipitation and mass spectrometry, CTL assays (both ELISA and Flow based) and IHC.

At the very basics of all our experiments is ensuring a proper and uniform lethal irradiation of modified tumor cells so that they can be used as vaccines and do not proliferate and result in tumor themselves.

Materials and Methods:

1. Transfection of Tumor cells : ID8 (fast) cells were plated in PEImax coated dishes and transfected with constructs that modulate the nature of the proteins synthesized by the cells.

2. Irradiation of Tumor cells : Since we are using a very aggressive murine MOSE sub-line called ID8 (fast) that is not only cisplatin resistant but is also able to withstand high levels of radiation (e.g., 60Gy radiation doesn't even stop proliferation), we need a very uniform and high level of irradiation to kill these cells (150 Gy), while keeping the protein synthesis and antigen presenting machineries of the cell intact. We performed irradiation with both Cs and X-ray irradiators.

3. In vivo immunization : We injected 1e6 irradiated cells i.p. to confirm that the cells were lethally irradiated and did not cause any tumor growth.

Results :

We were also able to lethally irradiate the tumor cells with a Cesium irradiator, which uses ^{137}Cesium to generate gamma rays. However, wherease we were able to lethally irradiate the cells with this irradiator, the tumor cells in suspension in tubes tended to settle down very fast, which puts into question the uniformity of irradiation. Using the X-ray irradiator, on the other hand, ensured highly uniform irradiation with cell being in culture medium in plates and the data obtained using this irradiator was very consistent and satisfactory. At 160 kVp (in free space), X-rays have more than enough penetration power to achieve the desired results for our experiments and yet requires much less shielding (Fig. 1).

The irradiated cells did not produce any tumor even in 120 days post injection, while live tumor cells even when injected subcutaneously, produced both local and metastatic tumors and all unvaccinated mice challenged with live tumor cells died within 49 days post tumor inoculation (Fig. 2).

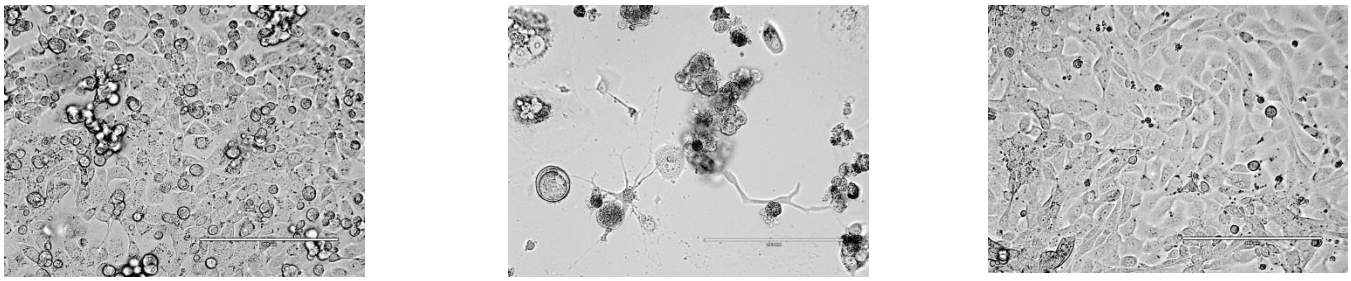

ID8(f)-150Gy-24h post irradiation ID8(f)-150Gy-15d post irradiation ID8(f) control

Fig. 1: Effect of Irradiation on Tumor Cell Survival with the X-Ray Irradiator

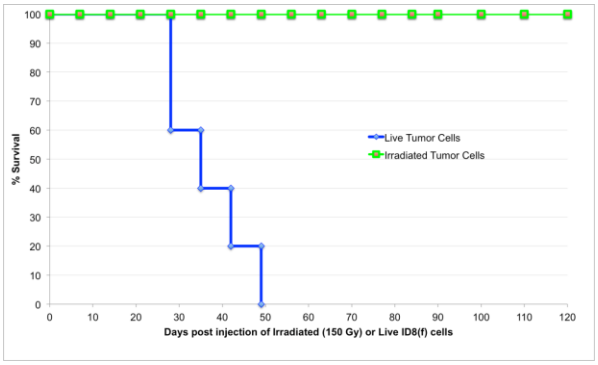

Fig. 2: ID8 Cells that Were Lethally Irradiated with the X-Ray Irradiator Don't Cause Tumor Growth.

Cancer Cell Organoid Core Experience in Transition to the X-ray irradiator

Pamela Cheung, Ph.D. and Stuart Aaronson, M.D.

The CCOC (Cancer Cell Organoid Core) is tasked with the generation of organotypic cell lines from human surgical specimens. The Standard Operating Procedure used for the propagation and maintenance of these cell lines requires the irradiation of the immortalized mouse embryonic fibroblast line, 3T3-J2, a subclone of 3T3-Swiss Albino cell line. The cells were previously irradiated in suspension in 50mls of DMEM (Dulbecco's Modified Eagle Medium) with 10% Fetal Calf Serum, 100 I.U./mL penicillin and 100μg/mL streptomycin, in a 50ml Falcon Tube. The cells were irradiated with the Cesium (gamma) source at 3000 rads (position 3, outer most position), and then used for the production of conditioned medium as a component of the multicomponent growth media. The irradiation of the 3T3-J2 cells elicits release of molecules into the media beneficial for growth of organotypic cell lines, and also renders the 3T3-J2 cells non-replicative.

Because of the planned decommission of the Cesium source irradiator and its replacement with the X-Ray irradiator, we investigated the impact of the different irradiation methods on our SOP. Previous research in mice (Comp Med. 2015 Jun; 65(3): 165–172) indicated while ablation of bone marrow was comparable using either source, distinct physiological responses were observed with reconstitution of specific cell types after irradiation. Thus, we compared effects on 3T3-J2 viability and growth in response to X-Ray vs gamma irradiation, as well as the effects on organotypic lines of conditioned media generated by these two approaches.

The setup of the X-Ray irradiator results in distribution of irradiation into a much more focused plane and area than with the Cesium source. Thus, we switched the container for cells in suspension from a 50ml Falcon Tube to a T75 non-adherent low-binding cell culture flask. We observed further that the irradiation time was more than doubled using the X-Ray irradiator for the same 3000 rads dose. After replating 3T3-J2 cells, the morphology of irradiated cells using either method was comparable, and there were no observable differences in cell death. However, tryspinization and replating of treated cells after 3 days revealed that gamma irradiated cells were able to adhere to the new cell culture dish, while X-Ray irradiated cells were not able to do so, indicating great cell injury with the latter.

Conditioned media generated using either irradiation source was able to support growth of our organotypic cell lines without observable morphological differences, and growth rates were also comparable. Because of the undefined nature of the molecules secreted by the 3T3-J2 line, and the necessity of these factors for maintenance and long-term propagation of our organotypic lines, it is still possible that there may be differences in the ability to maintain long term cultures of these cell lines.

Investigating the enhancing effects of combining radiation with oncolytic Newcastle Disease Virus (NDV) therapy in a murine melanoma model

Gayathri Vijayakumar, Peter Palese, Peter Goff
Department of Microbiology
Icahn School of Medicine at Mount Sinai

Introduction

Newcastle disease virus (NDV) has been previously demonstrated to possess significant oncolytic activity against mammalian cancers, and is considered a promising agent for cancer therapy due to its tumor-selective cell killing properties. NDV selectively replicates in cancer cells inducing cell death and stimulates innate and adaptive immune responses against tumor cells. Radiotherapy is a well established modality in cancer treatment and here we seek to explore whether rNDVs could serve as potential radiosensitizers, to enhance cancer killing by combined multimodality therapy.
The oncolytic activity of rNDV-LaSota-L289A-WT and rNDV-LaSota-L289A-mIL12, in combination with localized tumor irradiation and checkpoint inhibitors is studied in a B16-F10 melanoma mouse syngeneic tumor model. B16-F10 melanoma cells are injected into the hind flank of mice. Once tumors reach a predefined tumor size (below humane endpoint), tumor bearing mice receive intraperitoneal injections of checkpoint inhibitors and intratumoral injections of rNDV-LaSota-WT or rNDV-LaSota-mIL12 or control PBS either with or without localized radiotherapy. The treated mice are then monitored for tumor regression/clearance. The experimental groups include untreated tumor-bearing mice and tumor-bearing mice receiving intratumoral injections of rNDV-LaSota, rNDV-LaSota-mIL12 and PBS as control.

Experimental outline

For the B16-F10 model, tumors are implanted by injection of 2×10^5 cells in the right flank intradermally on day 0 and 1×10^5 cells in the left flank on day 4. On day 10, mice are irradiated with various doses of radiation ranging from 4 to 20Gy. Subsequently, on days 10, 12, 14, 16 and 18, mice are treated with intratumoral injections of 1×10^7 plaque-forming units (PFU) of NDV in PBS in a total volume of 100 ml and intraperitoneally with anti–CTLA-4 antibody (100 mg in 100 ml) or anti-PD1 (200mg in 100ml). The animals are euthanized for signs of distress or when the total tumor volume reaches 1000 mm^3.

Results and Discussion:

We observed that the NDV WT+20Gy cohort did the best in terms of complete remissions on the treated side as shown below.

The use of the X-Ray irradiator instead of the cesium irradiator facilitated studies of this scale.

NDV + 20Gy treatment cohort seems to exhibit the maximum tumor volume regressions

Group	N	Treatment	Dose	ROA
1	10	ANTI-PD1	200ug	IP
2	10	20 GY + ANTI-PD1	200ug	IP
3	10	4 GY x5 + ANTI-PD1	200ug	IP
4	10	NDV-WT + ANTI-PD1	200ug 1 × 10⁷ PFU	IP IT
5	10	20 GY + NDV-WT + ANTI-PD1	200ug 1 × 10⁷ PFU	IP IT
6	10	4 GY x5 + NDV-WT + ANTI-PD1	200ug 1 × 10⁷ PFU	IP IT

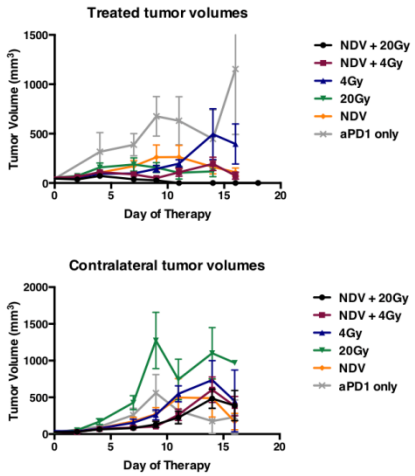

References:

1. Zamarin D, Vigil A, Kelly K, García-Sastre A, Fong Y. Genetically engineered Newcastle disease virus for malignant melanoma therapy. Gene Ther. 2009 Jun;16(6):796-804. doi: 10.1038/gt.2009.14. PubMed PMID: 19242529; PubMed Central PMCID: PMC2882235.
2. Zamarin D, Martínez-Sobrido L, Kelly K, Mansour M, Sheng G, Vigil A, García-Sastre A, Palese P, Fong Y. Enhancement of oncolytic properties of recombinant newcastle disease virus through antagonism of cellular innate immune responses. Mol Ther. 2009 Apr;17(4):697-706. doi: 10.1038/mt.2008.286. PubMedPMID: 19209145; PubMed Central PMCID: PMC2835121.
3. Vigil A, Martinez O, Chua MA, García-Sastre A. Recombinant Newcastle disease virus as a vaccine vector for cancer therapy. Mol Ther. 2008 Nov;16(11):1883-90. doi: 10.1038/mt.2008.181. PubMed PMID: 18714310; PubMed Central PMCID: PMC2878970.
4. Vigil A, Park MS, Martinez O, Chua MA, Xiao S, Cros JF, Martínez-Sobrido L, Woo SL, García-Sastre A. Use of reverse genetics to enhance the oncolytic properties of Newcastle disease virus. Cancer Res. 2007 Sep 1;67(17):8285-92.PubMed PMID: 17804743.

Comparisons of Using Cesium and X-ray as Sources of Irradiation in Blood Bank Operation

Jeffrey S. Jhang, MD and Suzanne Arinsburg, DO

Department of Pathology, Blood Bank and Transfusion Services, Mount Sinai Hospital, New York, NY

Introduction:

The purpose of this report is to share Mount Sinai Blood Bank's experiences with other institutions who may want to follow the same path. This section describes various issues that need to be reviewed for the migration from gamma irradiators to X-ray irradiators. Specific issues regarding technical considerations of X-ray irradiators, such as self-cooling and self-shielding, are explained. The cost comparison analyses between the two types of irradiators, including the cost for regulatory compliance, are presented. Since RadSource RS-3400 is approved by the FDA for blood irradiation, reliability studies of the unit were needed. The unit has been used for irradiation for the last 15 months, irradiating more than 9,000 bags of blood without any downtime. X-ray irradiators do not have decay problems and are much more efficient. For the X-ray irradiator one could irradiate 6 canisters, each containing 1-2 bags of blood, for a total irradiation time of five minutes. For the gamma irradiator one is limited to 2 bags of blood and a 9 minute irradiation time. Installation, training, validation, daily operation and preventive maintenance did not present an obstacle to successful migration. This migration did not affect patient care in any way, and it created a safe and relaxed environment for the blood bank staff to work without being worried.

Transfusion Associated Graft-versus-Host Disease (TA-GVHD):

Clinical Presentation: TA-GVHD is an adverse reaction to transfusion of a blood product containing lymphocytes. TA-GVHD is a clinical syndrome occurring within a few days to weeks after transfusion of a blood component with immunocompetent lymphocytes. It is characterized by one or more of the following: rash: erythematous, maculopapular eruption centrally that spreads to extremities and may, in severe cases, progress to generalized erythroderma and hemorrhagic bullous formation; diarrhea; fever; hepatomegaly and liver dysfunction (elevated liver enzymes); marrow aplasia with pancytopenia. There is a characteristic histological appearance of skin or liver biopsy. Unlike GVHD after an allogeneic hematopoietic transplantation, which has a mortality of 20-25%, TA-GVHD is associated with 90-100% mortality. The incidence is unknown due to under-recognition, under-reporting, and overlap with other reactions. TA-GVHD is a clinical diagnosis, but detection of donor lymphocytes confirms the diagnosis.

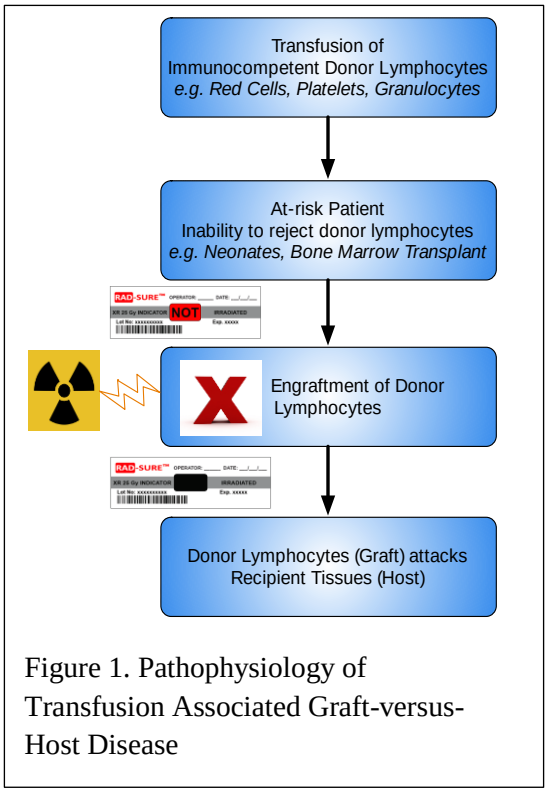

Figure 1. Pathophysiology of Transfusion Associated Graft-versus-Host Disease

Pathophysiology: The pathophysiology of TA-GVHD is the transfusion of immunocompetent lymphocytes in whole blood, packed red cells, or granulocytes into an at-risk recipient who is not able to reject the donor lymphocytes (**Figure 1**). Those at high risk include fetuses (intrauterine transfusion), neonates, recipients of hematopoietic progenitor cell transplants, and patients with inherited immune deficiencies (e.g. DiGeorge Syndrome, Severe combined immunodeficiency syndrome). The donor lymphocytes are able to proliferate and attack the recipient tissues leading to the constellation of findings. Another high-risk situation is a population with high HLA homogeneity in a population, as found in Japan. The HLA homogeneity can lead to a donor who is homozygous for one HLA haplotype and a recipient who is heterozygous for the same HLA haplotype. In this case, the recipient does not recognize the donor lymphocytes as foreign and does not reject the lymphocytes. However, the donor lymphocytes recognize the recipient as foreign.

Prevention: Leukoreduction is not sufficient to prevent TA-GVHD. Gamma irradiation to the center of the irradiation field with 25 Gy of □-irradiation inactivates lymphocytes by crosslinking DNA and preventing proliferation. Irradiation sources include X-ray (**Figure 2a**), cesium-137 (**Figure 2b**), cobalt-60, and linear accelerators. Quality control for each unit is performed to ensure that the proper irradiation dose was delivered (**Figure 2c**). Universal irradiation has not been widely adopted because the ionizing radiation harms red cells and can lead to accelerated efflux of potassium from red cells, decreased red cell survival, and a shorted expiration date to 28 days or the original expiration, whichever is shorter. A non-irradiation strategy that was recently FDA approved for prevention of TA-GVHD utilizes photochemical treatment with a chelating agent (amotosalen) followed by ultraviolet light exposure to cross-link DNA, thereby preventing donor lymphocyte proliferation.

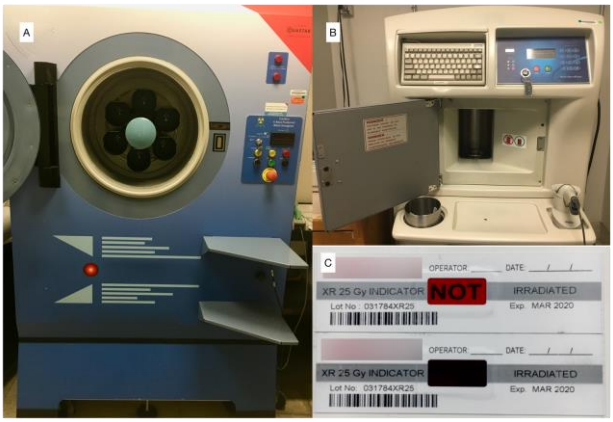

Figure 2. A. XR Irradiator B. Cesium Irradiator C. Quality Indicator

Switching from Cesium-137 to X-ray Irradiation:

Rationale: There have been many incidents in which terror groups planned to use high activity radioactive sources for malicious purposes. In 1987 an incident occurred in Brazil where 40 tons of radioactive waste were produced from the dispersal of 80 grams of cesium chloride power. Even though this was an accident, it demonstrated that if a similar source were to be used maliciously and purposely as a RDD in a densely populated area such as New York City, the result would be catastrophic. Most importantly, some Blood Bank staff are concerned that working in an area with a high activity radioactive source makes them a target for potential kidnapping or hijacking. Globally, Norway and France have removed all their Cesium irradiators. Japan is has removed 80% of its cesium irradiators already.

Cost-Benefit Analysis XR vs. Cs-137: A financial cost-benefit analysis was performed to compare Cs-137 vs. X- Ray. Acquisition, site preparation, and preventive maintenance costs were on the same order of magnitude. The disadvantage of Cs-137 was the increase cost of the Cs source, but the lifespan of an XR is ~12 years. The major disadvantage of Cs is the cost of disposal of the source (~ $200,000), as well as the cost of licensing, FBI background checks, and regulatory compliance and inspection.

Table 1. Cs-137 versus C-ray irradiator Financial Comparison (Courtesy of the University of Wisconsin Cost-Benefit Analysis of Switching from Cesium-Chloride Blood Irradiators to X-ray Blood Irradiators Prepared for GTRI and NNSA)

	Cs-137 Irradiator	**X-ray Irradiator**
Purchase Price	$160.000-$325,000 Est. $242,500	$160.000-$240,000 Est. $220,000
Site Preparation	$7,500	$0 -3,600
Licensing Costs	$15,400	$2,500
FBI Background check	$3,800	None
Transportation+ Disposal	$200,000	$2,500
Life	Source replacement every ~30 years ($150,000)	Tube replacement every ~12 years ($20,000); The life span of X-ray machine is ~12 years
	After 10 years, the cost to keep is ~same	
PM Cost per year	~$10,000 (RMS, PM, dose map)	$17,000 (warranty)
Regulatory Inspection	Yes, annually	None
Irradiation Time per Unit Dose	Increasing due to decay of the source	Constant

Selecting an XR Irradiator:

Regulatory: The device must be approved by the FDA for irradiation of blood products for allergenic transfusion.

Physical Plant: The elements for selecting an XR irradiator was based on the physical, electric, heating ventilation and air conditioning, and internet connectivity. The dimensions had to fit in the existing space. Our facilities department was consulted on 1) the amount of weight the floor could bear and 2) whether the device required appropriate electricity to be wired. One of the major factors in selecting the device was whether the instrument was self-cooling or if it required a water source of certain hardness. We chose the RS-3400, which is self-cooled. At the commissioning of the unit, 12 gallons of demineralized water was used to cool off the machine. The demineralized water is checked during preventive maintenance to see if it needs to be replaced. Construction costs of installing and routing the plumbing for cooling would increase the cost by $50,000 for our site preparation since we did not have a water source of the appropriate grade. Despite being self-cooled, the facility needs to evaluate whether the space can vent the appropriate amount of heat from the device. The X-ray irradiator should be in a room with air conditioning to better dissipate heat.

Operations: The throughput and medical technologist labor needed to fit within the operations of the blood bank. Therefore, the irradiation time, number of canisters per run, numbers of units per canister was considered to maximize the number of units irradiated in one run. Special compatibility, such as compatibility of syringes for pediatric transfusions were also looked upon as favorable. Ease of use, the user interface, barcode scanning, instrument-to-blood bank information system interfacings were all considered the selection. Our selection was a self-cooling unit able to have 6 canisters with 1-2 units per canister and a 5 minute cycle time. This was a significant improvement over our Cs irradiator, which irradiated 2 units with an almost 9 minute cycle time.

Required electricity and water for installation

Physical Plant	Modification of the physical plant was not required
Electricity	220 V AC was wired
Ventilation	Although the device was self-cooled; additional small mobile air conditioning unit added next to the X-ray generator for better heat removal
Instrument	Appropriate connections according to vendor checklist was completed and accepted by the blood bank director
Water	11 gallons of distilled water are required (only once).

Operational Qualification

- Dose delivery verified by RADCal radiation ion chamber.
- Validation plan executed in triplicate using expired blood products
    - Rad Sure indications applied to product before irradiation occurred and confirmed that indicator turned black afterwards
    - Temperature of blood products before and after irradiation
    - Irradiator timer will be verified for the set time using a calibrated stopwatch
    - Alerts are monitored for any problems with the unit using the multiple failure detectors that continuously monitor the irradiation cycle
    - Scanner program collects the data(product number, product code & Radsoure tag lot number that is scanned
    - Data can be downloaded and reviewed
    - User can document that the exposure dose was correct.

Performance Qualification

- Must meet the requirements will deliver 25 Gy as a center dose to a fully loaded canister and no more than 50 Gy. The dose distribution measurements are performed semi-annually. The manufacturer sends the TLDs to MD Anderson Cancer Center to be analyzed.
- Irradiation validation logs will be completed concurrently with performing the scenarios
- The dose and run time is associated with reach product in the run.
- Temperature of red blood cells will remain in the range of 1-10 °C during irradiation cycle
- Temperature of platelets will remain in the range of 20-24 °C during irradiation cycle
- Rad-Sure indicator will appear black after a cycle

Experience:

In order for the unit not to have any downtime, it is strongly recommended that the room has air conditioning. The output heat from the unit must be vented to cool down the X-ray generator. An additional mobile AC unit next to the X-ray generator would be an excellent idea, especially for occasions when the workload is very high. The instrument installation was complicated by the large heat output from the device which was higher than anticipated. This required air conditioning to be installed to maintain the appropriate temperature. Training of a super user at the manufacturer's facility, training of on-site users, and validation was completed within one month of installation qualification. Our facility provides ~25,000 red cell and ~8,000 apheresis platelet units (almost all irradiated by blood collection facility) annually. We have been using the instrument for 15 months and have irradiated 9,325 packed red blood cell units and 71 apheresis platelet units. Although there were some issues with the reliability of X-ray irradiators 10 years ago, the technology has improved tremendously and the new units have excellent reliability. Our facility has not experienced any overheating and no service calls to the manufacturer have been made for repairs. A stress test prior to using the X-ray as our sole irradiator showed that the device can handle irradiation of more than 100 units a day reliably. Our medical technologists find it easy to use and maintain and the throughput is more than adequate for our operations. The only enhancement that we would like develop is an interface from the device's tablet user interface to the blood bank information system. Our understanding is that such an enhancement can be custom-designed.

Summary: X-ray irradiator technology has improved its reliability in recent years. X-ray devices with self-cooling and self-shielding are highly recommended. X-ray devices must be FDA approved. The X-ray irradiator was justified by improved safety, cost, and efficiency, as well as decreased regulatory oversight and security measures. Installation, training, validation, daily operation and preventive maintenance did not present any obstacles to successful implementation. Despite concerns based on earlier X-ray devices, our facility did not require any service calls and had no overheating, X-ray tube burnout, or power supply failure after irradiation of over 9,300 blood products in 15 months.

Conclusion and Recommendations

Jacob Kamen Ph.D.
Icahn School of Medicine at Mount Sinai, New York, NY, USA

In this report, we have summarized the effort we have made since 2010 to reduce and eventually remove the cesium irradiators from Mount Sinai with the collaboration with many other institutions, regulatory agencies, law enforcement agencies and US government agencies. Since the reliable alternative technologies are available now, we could phase out the cesium irradiators to eliminate the risk of using the high activity radioactive sources as possible Weapon of Mass Disruption (WMD). We do appreciate the help from US-DOE for the OSRP program for disposal of Cesium Irradiators, the NNSA-ORS (GTRI) for security enhancement as well as the US-DOE-PNNL for CIRP for assistant with X-ray irradiator in the last 8 years. We highly recommend all institutions to take advantage of the help these programs offer.

Blood irradiation:

X-ray blood irradiator was FDA approved and available at the market many years ago. Since blood x-ray irradiators are FDA approved to be used to prevent Ta-GVHD diseases, we only have to consider the reliability of the x-ray units. Early x-ray blood irradiators were less reliable, which was problematic for blood centers which have a high throughput. There were many operational issues due to a more complicated mechanical design and the challenge to dissipate the heat efficiently. With the progress of technologies, there are more models of x-ray blood irradiators available, and the reliability has been improved significantly. Newer models come with a longer life span of the x-ray tubes and less downtime. Before disposing its cesium irradiator, Mount Sinai decided to run the x-ray irradiator and gamma ray irradiator side by side for almost one year to see if the x-ray blood irradiator could be a satisfactory replacement for the cesium irradiator. We also made back up plans in case the x-ray machine fails. We put the unit under the stress to evaluate its reliability. We increased the number of bags to be irradiated per day by factor of 4-5, and the machine was able to handle it. During the side by side comparison period, the x-ray machine experienced a sudden electric shutdown, the machine was rebooted and no issues were observed. We never had to use our back up plans for more than a year of operation so far and the patient services have never been affected. In fact, x-ray blood irradiators have proven to be far superior in performance than their cesium-137 counterparts: they consistently take less than 5 minutes to irradiate six blood bags, compared to an aging cesium source, which can take up to 12 minutes to irradiate just four bags. As a high throughput facility for blood products, the conversion to x-ray has increased our overall capabilities for sterilizing blood products. At this time we are confident that all the gamma blood irradiator could

be easily replaced by X-ray irradiators. Since transitioning to x-ray technology in March 2017, our quality of care for sterilizing blood has remained the same and we operate in both a medical environment and high-profile city with much less risk.

Research Irradiation:

As for research irradiators, each institution has to look at their own applications. Research x-ray irradiators with peak energy up to several hundred kVp cannot be used to irradiator large animals such dogs or cats, they are used to irradiate cells and small animals like rodents. All the research applications at the Icahn school of Medicine at Mount Sinai either are cells or small animals for different purposes. We have compiled in this report how researchers were able to migrate successfully to x-ray irradiators. The key to success is to work with health physicists / medical physicists to make sure the accurate dose is delivered. In the applications of x-ray irradiators the beam profile could be either hardened or softened to get accurate dose to the target.

Some final points to consider:

- Cs-137 originally not engineered for irradiation purposes rather it was one of the by-product from nuclear power plant operation.
- The dose distribution in an x-ray irradiator is much more homogeneous than in a cesium irradiator.
- The dose deviation in an x-ray irradiator is much smaller than in a cesium irradiator.
- X-ray irradiators will not be covered under 10CFR part 37 regulations and therefore there will not be any need to have any FBI background check on the staff incurring security cost and licensing cost.
- Institutions should use the US government program called “Off-site Source Recovery Program” (https://osrp.lanl.gov) and the Cesium Irradiator Replacement Program (https://www.energy.gov/sites/prod/files/migrated/nnsa/2017/11/f45/ors_cirp_brochure_r18_web.pdf) to dispose and replace high activity cesium sources. In the near future these sources may become commercially disposable and it may then cost about $200,000 to dispose each cesium irradiator.
- Institution’s leadership and management should check their insurance coverage very carefully for radioactive decontamination cost from a possible dirty bomb incident. They must remember from the experience in Brazil that 80 grams of cesium powder resulted in more than 40 tons of radioactive waste.
- The governments of Norway, France and Japan must be commended for their decisions to remove such sources from their societies. Perhaps this is one way we could help to fight and reduce the risk of malicious use of high activity radioactive sources.
- It is recommended to get a self-cooling and self-shielded x-ray irradiator.
- If possible, we recommend to setup for the manufacturer to be able to remotely see the error messages on research irradiator to reduce the down time.

- For x-ray blood irradiators, it is recommended someone from the Clinical Engineering Department or the operators go to the company and get training on how to troubleshoot the irradiator.
- For blood x-ray irradiators, an air conditioned room is preferred, otherwise, you can use a fan or portable AC to maintain the room temperature and facilitate the heat dissipation from the irradiator.
- For x-ray research irradiator, make sure the water supply is clean and install a pre-filter for water intake.

Mount
Sinai